

**CALCULATING THE NORMALISED DETERMINANT FUNCTION  
USING NON-LINEAR MODELS IN MICROWAVE OFFICE**

Sumiya Sultan

Bachelor of Engineering (Honours)  
with a major in Electronics Engineering



**MACQUARIE**  
University

Department of Electronic Engineering  
Macquarie University

June, 6 2016

Supervisor: Professor Anthony Parker



## **ACKNOWLEDGMENTS**

I would like to acknowledge the help of my academic supervisor Professor Anthony Parker and key industry engineers, Bryan Schwitter and Tony Fattorini from MACOM Technology Solutions. I am grateful to Bryan Schwitter and Tony Fattorini for sharing their preliminary version of their work.



## **STATEMENT OF CANDIDATE**

I, Sumiya Sultan, declare that this report, submitted as part of the requirement for the award of Bachelor of Engineering (Honours) in the Department of Electronic Engineering, Macquarie University, is entirely my own work unless otherwise referenced or acknowledged. This document has not been submitted for qualification or assessment at any other academic institution.

Student's Name: Sumiya Sultan

Student's Signature: SUMIYA SULTAN

Date: 6 June, 2016



## ABSTRACT

Stability of a circuit is a very important design criteria. Microwave designers commonly use the well known Linvill or Rollett criteria, known as B or K criteria to determine the stability of an N-port network. These criteria are limited to its accuracy and fail in many cases. A rigorous method of testing such as the Normalised Determinant Function (NDF) is required before the B or K criteria is applied. The Normalised Determinant Function is a robust test of circuit stability but can be complicated to implement in a circuit simulator because it requires access to all active controlled sources in a circuit and multiple simulations. Access to the necessary controlled sources has recently been implemented in a non-linear model (Meerkat pHEMT model) for the first time, but some problems remain with the implementation of this useful feature. This thesis provides further work to mathematically analyse and simplify the NDF analysis technique to implement in small signal models that will later on aid Macquarie University's industry partner, MACOM Technology Solutions with the NDF implementation in their preferred Meerkat pHEMT model.



# Contents

Acknowledgments	iii
Abstract	vii
Table of Contents	ix
List of Figures	x
<b>1 Introduction</b>	<b>1</b>
1.1 Normalised Determinant Function . . . . .	2
1.2 Synopsis . . . . .	3
<b>2 Background</b>	<b>5</b>
2.1 What is the NDF? . . . . .	5
2.2 How is the NDF used to determine stability? . . . . .	5
2.3 How is the NDF calculated? . . . . .	8
2.4 Microwave Office AWR Simulator . . . . .	12
<b>3 Determining the Stability of N-Port Networks</b>	<b>13</b>
3.1 Calculating NDF for a Single Three-Port FET Model . . . . .	18
<b>4 Small Signal Implementation in circuit simulator AWR</b>	<b>21</b>
4.1 Modification of the existing circuit model . . . . .	25
4.2 Implementation of the two control sources in the switching model . . . . .	35
<b>5 Comparison of analysis approach</b>	<b>39</b>
5.1 Results for Single FET single source . . . . .	40
5.2 Results for Two FETs single source . . . . .	41
5.3 Results for Two FET, Two Control Source Model . . . . .	43
5.4 Further Three FET model implementation . . . . .	46
<b>6 Conclusion</b>	<b>49</b>
<b>7 Abbreviations</b>	<b>51</b>

<b>A Project Attendance Form</b>	<b>53</b>
<b>B Related Paper</b>	<b>55</b>
<b>Bibliography</b>	<b>59</b>

# List of Figures

2.1	Polar plot of NDF (This figure is obtained from [11]) . . . . .	6
2.2	Frequency response of NDF plot (This figure is obtained from [10]) . . . . .	6
2.3	Two-Port representation for calculation of NDF . . . . .	8
2.4	Passively terminated N-Port linear network with a voltage controlled current source (This figure is obtained from [10]) . . . . .	10
2.5	Passively terminated N-Port network of Figure 2.4 where the current source is controlled by an external voltage, $v_{ext}$ instead of $v_{13}$ . . . . .	10
3.1	Introducing a second source in the passively terminated Two-Port network	13
3.2	Three-Port FET model with an additional control source . . . . .	18
4.1	Top Level Circuit model diagram in AWR (obtained from MACOM) . . . . .	22
4.2	Second Level Circuit model diagram in AWR . . . . .	22
4.3	Bottom Level Circuit model diagram in AWR . . . . .	23
4.4	Filter circuit as shown in the top Level of AWR circuit model . . . . .	23
4.5	Switching block included within the individual FET . . . . .	24
4.6	Modified circuit model . . . . .	27
4.7	Modified circuit model . . . . .	28
4.8	Magnitude of NDF versus Magnitude of NDF calculated using equation 4.7	29
4.9	Angle of NDF versus Angle of NDF calculated using equation 4.7 . . . . .	30
4.10	NDF Encirclements around the origin representing zeroes on the RHP . . . . .	31
4.11	The number of encirclements around the origin . . . . .	31
4.12	The modified circuit model to include a second FET . . . . .	32
4.13	The modified circuit model to include a second LRC filter circuit . . . . .	33
4.14	NDF Encirclement trajectory on a polar plot when $g_m = 0.12$ . . . . .	34
4.15	Number of encirclements and zeroes on the RHP when $g_m = 0.12$ . . . . .	34
4.16	Two FET two control source FET model with a shared switching block . . . . .	35
4.17	Two FET two control source model with individual switching blocks . . . . .	36
4.18	Control source with gate-drain connections . . . . .	37
4.19	Control source with gate-source connections . . . . .	37
5.1	NDF Encirclement trajectory on a polar plot when $g_m = -0.05$ . . . . .	40
5.2	Number of encirclements when $g_m = -0.05$ . . . . .	40
5.3	NDF Encirclement trajectory on a polar plot when $g_m = 0.042$ . . . . .	40

---

5.4	Number of encirclements when $g_m = 0.042$ . . . . .	40
5.5	NDF Encirclement trajectory on a polar plot when $g_m = -0.05$ . . . . .	41
5.6	Number of encirclements when $g_m = -0.05$ . . . . .	41
5.7	NDF Encirclement trajectory on a polar plot when $g_m = 0.042$ . . . . .	41
5.8	Number of encirclements when $g_m = 0.042$ . . . . .	41
5.9	Polar trajectory plot by sweeping $\omega$ from 0 to $-\infty$ . . . . .	43
5.10	NDF encirclement plot by sweeping $\omega$ from 0 to $-\infty$ . . . . .	44
5.11	Polar trajectory plot by sweeping $\omega$ from 0 to $-\infty$ . . . . .	45
5.12	NDF encirclement plot by sweeping $\omega$ from 0 to $-\infty$ . . . . .	46
5.13	Three FET model for NDF analysis . . . . .	47
5.14	NDF polar trajectory plot by sweeping $\omega$ from 0 to $-\infty$ . . . . .	47
5.15	NDF encirclement plot by sweeping $\omega$ from 0 to $-\infty$ . . . . .	48

# Chapter 1

## Introduction

Design engineers are constantly faced by the challenge of determining stability of a circuit before it is sent out for fabrication. Unstable circuits can oscillate and fail to meet its purpose. Over the last 50 years, several tests have been derived for determining the unconditional stability of two-port networks. These tests are used to determine the possibility of finding a set of passive terminations that will cause the terminated two-port to have unstable characteristic frequencies (poles).

The well known Linvill and Rollett stability criteria also known as the B and K criteria respectively, are usually used by designers, to determine stability of microwave circuits by reducing the complicated N-node networks to two-ports between input and output and requiring that  $K > 1$  and  $|\Delta_s| < 1$  at all frequencies. Platzker *et al.* [6] prove that the approach undertaken by the microwave designers with its reliance on K is severely constraining in many cases. Rollett's, K stability criteria [12].

The K analysis does not hold in general, and fails in many cases where the unloaded circuits under investigation contain poles with positive real parts, i.e. poles in the right half plane (RHP). Rollett [8] recognises the limitation of using steady state analysis in investigating the stability of Two-Ports. This remains as a significant problem that the more recent publications, textbooks and software vendors have failed to highlight. Hence, the microwave designers have forgotten to take this into consideration altogether.

The failure of the B and K criteria stems from the fact that no universal determination of the stability of N-node networks can be made from the locations of the zeroes of the determinants of their reduced Two-Ports. They can be unstable even if all of the zeroes of these determinants have negative real parts. This failure is not dependent on the symmetry of the networks and can occur in both symmetric and nonsymmetric networks. Since the conditions for oscillations are the opposite of the conditions for stability, the notion that a circuit is always oscillatory at a frequency at which the imaginary part of its input or output admittance is zero provided the real part is negative, is also not correct. [11].

A proper statement of the Two-Port stability criteria involving K should be: An unloaded Two-port which has no poles in the RHP will remain stable when loaded externally at its input and output if and only if  $K > 1$  and  $|\Delta_s| < 1$  for all W. The approach of using

the K criteria to ensure stability in Two-Port networks is not very robust and hence its role is insignificant. It is limited to the investigation of loading which does not cause stable unloaded circuits to become unstable. The stability of the open circuit has to be ascertained by other means. [6]

A robust test such as the Normalized Determinant Function is required to ensure the stability of a network before the Linvill or Rollett stability criteria are used.

## 1.1 Normalised Determinant Function

The Normalised Determinant Function analysis technique looks for zeroes in the right half plane of the full network determinant. The complex quantity NDF is calculated for a given network along the frequency axis  $\omega$  from negative infinity to positive infinity and its locus is plotted in the complex plane. Once network stability is assured, then the B or K factor can be used to determine the port impedances under which stability is maintained [4].

The Normalised Determinant Function (NDF) is a robust test of circuit stability but can be complicated to implement in a circuit simulator because it required access to all the active controlled sources in a circuit and multiple simulations. Access to the necessary controlled sources has recently been implemented in a non-linear model (Meerkat pHEMT model) for the first time but some problems remain with the implementation of this useful feature.

As mentioned earlier, this thesis is an extension of the work of Wayne Struble and Aryeh Platzker [11]. Struble found a simple yet rigorous method of determining the stability of a linear N-Port network by first reducing it to a two port network. Before this was discovered, a common misunderstanding persisted that the B and K stability criteria can only be applied to linear two-port networks. This thesis is extended to first analyse what happens to the two port network NDF calculation when two dependent current sources are used in a linear model instead of the one source as defined in Struble's model. However, the design of the two port circuit is restricted to one common node to make the simplification easier. The initial findings of the mathematical analysis is shown in the latter section.

Later, implementation of the above findings is used in a non-linear FET model which is linearised using small signal model. The result of the thesis will aid in the implementation of the NDF in MACOM's more sophisticated and preferred Meerkat pHEMT model.

## 1.2 Synopsis

This thesis is based on a very narrow and specialised area of research to aid the implementation process of the NDF analysis in the design phase of circuits at MACOM Technology Solutions. Very little work has been done on this robust stability test NDF analysis and so the resources and references used in this thesis is limited. As stated earlier, engineers at MACOM, Tony Fattorini and Bryan Schwitter have jointly developed the small signal implementation of NDF analysis in some simple models, however, some problems remain with the implementation of this useful feature in the more sophisticated and preferred non-linear model, Meerkat pHEMT model. One of the problems that arises with the implementation of the NDF in the Meerkat pHEMT model is that the model consists of multiple control sources in one single pHEMT and the study by Struble [11] only looks at single control source transistors. This thesis is an extension to Struble's work and looks further into what the implications are in having multiple control sources and how it changes the NDF algorithm both algebraically and practically.

In this 10 week thesis project, most of the time, about 5 weeks was dedicated in developing the mathematical case for using a double voltage controlled current source (VCCS) FET model, the effort of which might not have been portrayed in its true essence due to the limitation of presenting a step by step mathematical analysis in this thesis. Next, the remaining amount of time was utilised to modify the circuit model obtained from MACOM, developed by Tony Fattorini and Bryan Schwitter, to ensure that the NDF stability analysis works with a single FET. Later, a comparative analysis is drawn between a single and a double FET model. The double FET model also has two separate parts to it where two different switching patterns are used. The two switching networks are used to control the VCCS by an external voltage source,  $v_{ext}$ . This phenomenon is described in details in the next chapter.

The results from this thesis can be used to aid the implementation of NDF in a more complex Meerkat pHEMT model. The calculation required for the NDF analysis and the concept of NDF and Return Ratios is introduced in the next chapter.

## Scope

This thesis looks at the NDF algorithm of having multiple control sources within the desired FET model used in MACOM. The case of having multiple control systems was not explored in any of Struble's [10] work so this thesis serves as an extension to Struble's work and looks at both the mathematical algorithm and practical implementation of NDF in a simple circuit model. The circuit model used does not contain real transistors and does not represent a fully complex network containing lumped elements. It is to be noted that the aim of the thesis is not to implement the full NDF stability analysis or provide an overall general solution of NDF analysis in any arbitrary circuits as it is outside of the scope of an Honours thesis since this demands much more time and expertise. The thesis does not look at writing scripts and macros that was initially suggested to facilitate ease of use in typical circuit design applications.

## Statement of Originality

This thesis is an extension to Struble's [10] work and such analysis to the best of my knowledge has not been carried out. The circuit model used in this thesis was not developed from scratch but was rather a modified version of the circuit model used at MACOM developed by Tony Fattorini and Bryan Schwitter. This circuit model was modified to suit the purposes of this thesis.

# Chapter 2

## Background

### 2.1 What is the NDF?

Platzker's normalized network determinant function NDF [6] is the ratio of the full network determinant, including all port terminations, and the resulting passive network determinant when all dependent sources (i.e. either voltage controlled or current controlled sources) contained within the network are set equal to zero.

$$NDF = \frac{\Delta}{\Delta_{0N}} \quad (2.1)$$

where  $\Delta_{0N}$  represents the determinant of a passive network and cannot contain any zeroes in the RHP. Therefore, zeroes in the RHP of the NDF must correspond to zeroes in the RHP of the full network determinant. This is similar to Bode's [3] definition of the Return Difference  $\frac{\Delta}{\Delta_0}$  for a single dependent source, where  $\Delta_0$  represents the network determinant when the dependent source is set to zero. Any linear network parameters such as Y, Z, H etc. can be used to calculate the above determinants. In this paper, admittance parameter Y is used for the mathematical analysis [10].

### 2.2 How is the NDF used to determine stability?

To determine stability, the complex quantity NDF is calculated for a given network along the frequency axis  $\omega$  from negative infinity to positive infinity and its locus is plotted in the complex plane if the locus of the NDF encircles the origin (0,0) in a counterclockwise direction, then the network determinant  $\Delta$  contains zeroes in the RHP. The number of encirclements is equal to the number of zeroes in the RHP. Platzker's test applies the Principle of the Argument theorem to a NDF to determine the number of zeroes in the RHP of the full network determinant (and thus poles of the network). Nyquist [5] has used the same theorem of encirclements for his stability analysis. From Routh [9] and Bode [3], it is known that if the determinant of a linear network contains any zeroes in the

RHP, including the frequency axis  $\omega$ , the network will be unstable, otherwise the network is stable [10].

Platzker's test [6] applies the Principle of the Argument theorem to a NDF to determine the number of zeroes in the RHP of the full network determinant (and thus poles of the network). This can be demonstrated by the two figures as shown below in figure 2.1 and figure 2.2

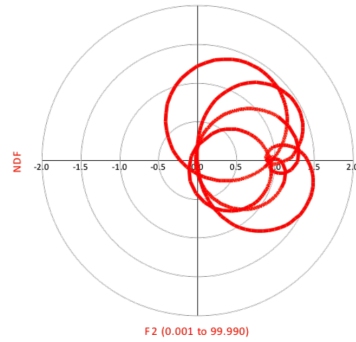


Figure 2.1: Polar plot of NDF (This figure is obtained from [11])

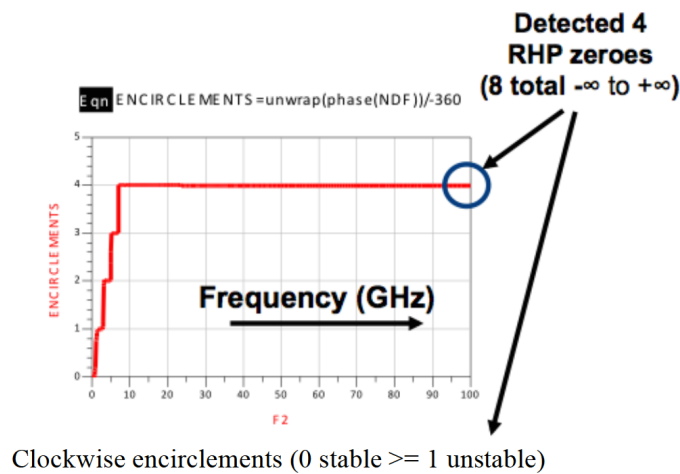


Figure 2.2: Frequency response of NDF plot (This figure is obtained from [10])

A stable network will always have a cumulative NDF phase/encirclement of zero. That is, sweeping  $\omega$  from  $-\infty$  to  $+\infty$  the plot will begin (by definition) and end at zero encirclements. It is unimportant if the encirclement plot rises above +1 or below -1 so long as it returns to 0 at  $\omega = +\infty$ .

When swept from  $\omega = -\infty$  to  $+\infty$ , an unstable network will have a cumulative NDF phase of some multiple of 2. Since, the NDF over negative frequencies is the complex conjugate of positive frequencies, one can look for encirclements from  $\omega = 0$  to  $+\infty$  only. This will always show half the encirclements. In the experimental part described in the latter sections of the thesis, the model is swept from  $\omega = 0$  to  $+\infty$  so, half the encirclements, i.e, multiples of unity can be observed.

From the above figure 2.1 and figure 2.2 it can be observed that the example model has four zeroes on the RHP, making the circuit unstable.

## 2.3 How is the NDF calculated?

The NDF analysis requires the calculation of the network determinants. There are three ways to calculate the network determinants.

1. Return Ratios
2. Current/Voltage Ratios
3. Network Admittances

**The mathematical analysis of the network determinants for the NDF calculation used in MACOM and this thesis is based on the first method, the Return Ratio method.**

The Return Ratio of a dependent source embedded within a network is calculated by replacing the dependent source, which is controlled by an internal voltage or current, with an identical source that is controlled by an external voltage or current. The stimulus from this new source will result in some amount of feedback to the controlling voltage or current of the original dependent source. The negative ratio of the voltage or current returned, to the external voltage or current stimulus, is the Return Ratio of the dependent source. The procedure used to calculate the NDF from Return Ratios (RRs) is described as follows.

The fastest approach employed by all NDF calculations is to reduce the network to a parallel connection of two networks, one totally passive and one totally active [10]. This is demonstrated in figure 2.3.

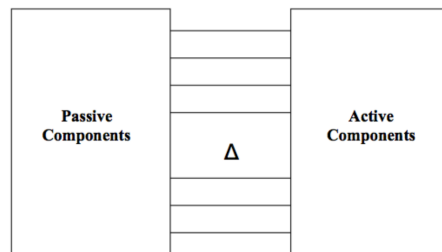


**Figure 2.3:** Two-Port representation for calculation of NDF

This reduces the number of nodes in the network and thus the sizes of the relevant network matrices that are used in the NDF calculation. The network cannot be reduced further than this due to the complication of potentially introducing zeroes in the RHP of  $\Delta_{0N}$ . This can result in pole-zero cancellation in the NDF, and thus its trajectory may not rotate around the origin (0,0) even when  $\Delta$  contains zeroes in the RHP.

In networks containing more than five dependent sources, the calculation of the NDF using commercially available circuit simulators is not straightforward and becomes quite

tedious. This is due to the limitation in the sizes of matrices that can be saved by the simulators for external calculations. To simplify this process, the alternative method of calculating NDF using the concept of Return Ratios has been developed.

### The Method of Calculating NDF using Return Ratios

The concept of Return Ratio (RR) was first introduced by Bode [3] and is defined as follows.

$$RR = \frac{\Delta}{\Delta_0} - 1 \quad (2.2)$$

where  $\Delta$  is the full network determinant and  $\Delta_0$  is the full network determinant where the dependent source is set to zero. For a network containing a single dependent source, the Return Ratio is equivalent to the NDF. The NDF for a single dependent source is as follows:

$$NDF = \frac{\Delta}{\Delta_0} = RR_1 + 1 \quad (2.3)$$

If the network contains more than one dependent source,  $\Delta_0$  may contain zeroes in the RHP due to other dependent sources, and a single Return Ratio calculation will not suffice to provide with a comprehensive assessment of stability of the circuit. However, the concept of Return Ratios can be extended to networks with N dependent sources by rearranging the previous equation into the form,

$$\Delta = (RR_1 + 1)\Delta_{01} \quad (2.4)$$

and realising that,

$$\Delta_{01} = (RR_2 + 1)\Delta_{02} \quad (2.5)$$

where  $RR_2$  is the Return Ratio of a second dependent source in the network with the first dependent source set to zero. By substituting the latter equation to the first, it is derived that

$$\Delta = (RR_1 + 1)(RR_2 + 1)\Delta_{02} \quad (2.6)$$

By continuous substitution,

$$\Delta = (RR_1 + 1)(RR_2 + 1)(RR_3 + 1)\dots(RR_N + 1)\Delta_{0N} \quad (2.7)$$

or,

$$NDF = (RR_1 + 1)(RR_2 + 1)(RR_3 + 1)\dots(RR_N + 1) \quad (2.8)$$

For each successive Return Ratio calculation  $RR_i$  ( $i = 2-N$ ), the network is physically changed by setting all previous dependent sources to zero.

### Return Ratio Calculations

The final step required to implement this rigorous stability test is to calculate the Return Ratio of any arbitrary dependent source within a known N-port network. This calculation is carried out by replacing the dependency factor of the dependent source from an internal voltage or current parameter to an identical external parameter. So, the dependent source is now controlled by an external voltage or current.

This can be demonstrated with an example in figure 2.4 and figure 2.5 where the first is a passively terminated N-port linear network with an internally controlled current source and the latter is the same network, the current source of which is controlled by an external voltage,  $v_{ext}$ .

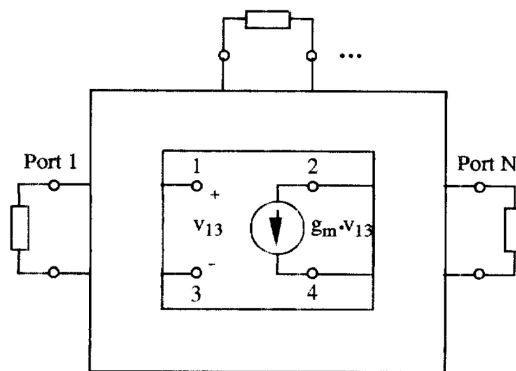


**Figure 2.4:** Passively terminated N-Port linear network with a voltage controlled current source (This figure is obtained from [10])

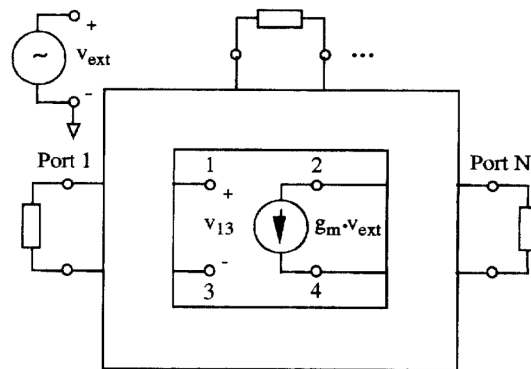


**Figure 2.5:** Passively terminated N-Port network of Figure 2.4 where the current source is controlled by an external voltage,  $v_{ext}$  instead of  $v_{13}$

Later, it has been derived by Platzker [6]

$$RR = -\frac{v_{13}}{v_{ext}}. \tag{2.9}$$

The proof of this simple equation is shown in great detail in [10]. It starts from pulling out the admittance matrix of the network. The Y representation is

$$Y(S)V(S) = I(S) \quad (2.10)$$

where  $s = \sigma + j\omega$ ,  $Y(S)$  is a  $n \times n$  matrix and  $I(S)$  and  $V(S)$ , are respectively excitation and response column vectors of size  $n$  where  $n$  is the number of nodes in the circuit. The Y matrix of the network shown in figure 2.4 is given by the matrix below.

$$\begin{pmatrix} y_{11} & y_{12} & y_{13} & y_{14} & \cdots & y_{1N} \\ y_{21} + g_m & y_{22} & y_{23} - g_m & y_{24} & \cdots & y_{2N} \\ y_{31} & y_{32} & y_{33} & y_{34} & \cdots & y_{3N} \\ y_{41} - g_m & y_{42} & y_{43} + g_m & y_{44} & \cdots & y_{4N} \\ \vdots & & & & \ddots & \\ y_{N1} & y_{N2} & y_{N3} & y_{N4} & \cdots & y_{NN} \end{pmatrix} \quad (2.11)$$

The next step is to write up the admittance, voltage and current equation of circuit model shown in figure 2.5. This is shown as follows.

$$\begin{bmatrix} y_{11} & y_{12} & y_{13} & y_{14} & \cdots & y_{1N} \\ y_{21} + g_m & y_{22} & y_{23} - g_m & y_{24} & \cdots & y_{2N} \\ y_{31} & y_{32} & y_{33} & y_{34} & \cdots & y_{3N} \\ y_{41} - g_m & y_{42} & y_{43} + g_m & y_{44} & \cdots & y_{4N} \\ \vdots & & & & \ddots & \\ y_{N1} & y_{N2} & y_{N3} & y_{N4} & \cdots & y_{NN} \end{bmatrix} \times \begin{bmatrix} v_1 \\ v_2 \\ v_3 \\ v_4 \\ \vdots \\ v_N \end{bmatrix} = \begin{bmatrix} i_1 \\ -g_m \cdot v_{ext} \\ i_3 \\ g_m \cdot v_{ext} \\ \vdots \\ i_N \end{bmatrix} \quad (2.12)$$

The matrix in equation (2.11) is the full network determinant and the network admittance shown in (2.12) represents  $Y_0$  when the dependent source with the transconductance value  $g_m$  is excited.

Since,  $RR = \left| \frac{Y}{Y_0} \right| - 1$ , the Return Ratio for the network is calculated and proved to be as Equation (2.9).

$$RR = -\frac{v_{13}}{v_{ext}}$$

This result is particularly useful to extend the work that this thesis presents. In order to solve the big  $n \times n$  matrices, there is a need to be familiar with solving matrices using the concept of partitioned matrices or more commonly known as block matrices. This concept is explained in [7].

## 2.4 Microwave Office AWR Simulator

The Microwave Office [1] is a comprehensive software solution for engineers and designers of all types of RF and microwave circuits starting from integrated microwave assemblies to monolithic microwave integrated circuits (MMICs). Microwave Office offers an intuitive user-interface which combined with its unique architecture software allows for seamless integration of powerful, innovative tools and technologies with application-specific tools based on the need of partner companies to bring their high-frequency designs to life. The capabilities of Microwave Office includes:

- Schematic/layout design entry
- Linear and non-linear circuit simulation
- EM analysis
- Synthesis, optimization and yield analysis
- Design rule checking/layout vs. schematic (DRC/LVS)
- Process design kits (PDKs) from a wide range of foundries

This thesis makes use of the basic capabilities of Microwave Office NI AWR Design Environment to enable schematic design entry, linear and non-linear circuit simulation. However, it also uses more advanced PDKs that have been obtained from MACOM for the purposes of the thesis.

A process design kit (PDK) is a set of files used within the semiconductor industry to model a fabrication process for the design tools used to design an integrated circuit. The PDK is created by the foundry defining a certain technology variation for their processes. The designers use the PDK to design, simulate, draw and verify the design before handing the design back to the foundry to produce chips [13].

Microwave Office AWR was used to modify the circuit model provided by MACOM. This tool combined with the knowledge acquired over the years of using this tool in the Engineering degree at Macquarie University and the experience of Anthony Parker and engineers at MACOM was required to carry out the small signal implementation of the two dependent source model of a FET that is discussed in the next chapter.

## Chapter 3

# Determining the Stability of N-Port Networks

The Two-port network model extracted from Struble's [10] work has been shown in Chapter 2. This mathematical study is an extension of the NDF analysis for N-port networks carried out by Struble using single current sources. This thesis is aimed to look at the implications of having multiple control sources within a FET to represent the realistic transistors used in MACOM's preferred Meerkat pHEMT model.

This thesis particularly looks at the implementation of a two dependent source model based on Struble's Two-Port network as shown in figure 2.5. The two control sources used in this model are voltage controlled current sources that are equal in magnitude but opposite in direction. This is represented in the figure 3.1.

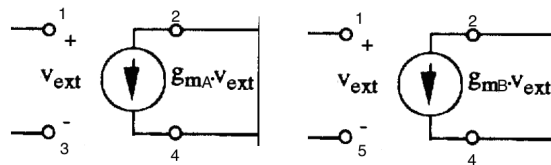


**Figure 3.1:** Introducing a second source in the passively terminated Two-Port network

This new model has been restricted to a common node, Node 1, as shown in figure 3.1. The next step in carrying out the mathematical NDF analysis is to work out the admittance matrix of the network and use it to find values for  $v_1$ ,  $v_3$  and  $v_5$ . equation 2.10  $Y(S) * V(S) = I(S)$  is used for these Return Ratio calculations that can be referred back to the previous chapter.

$$\begin{bmatrix} y_{11} & y_{12} & y_{13} & y_{14} & y_{15} \\ y_{21} + g_{mA} + g_{mB} & y_{22} & y_{23} - g_{mA} & y_{24} & y_{25} - g_{mB} \\ y_{31} & y_{32} & y_{33} & y_{34} & y_{35} \\ y_{41} - g_{mA} - g_{mB} & y_{42} & y_{43} + g_{mA} & y_{44} & y_{45} + g_{mB} \\ y_{51} & y_{52} & y_{53} & y_{54} & y_{55} \end{bmatrix} \times \begin{bmatrix} v_1 \\ v_2 \\ v_3 \\ v_4 \\ v_5 \end{bmatrix} = \begin{bmatrix} i_1 \\ i_2 \\ i_3 \\ i_4 \\ i_5 \end{bmatrix} \quad (3.1)$$

These equations are to be used in two different scenarios. These are as follows.

- Scenario 1: Each current source, i.e.  $g_{mA}$  and  $g_{mB}$  is excited and set to zero successively and the NDF calculated is based on the two return ratios obtained from each step in this two step process.
- Scenario 2: Both the sources are probed by an external stimulus, simultaneously and the NDF is calculated based on the Return Ratios obtained in one single step.

The aim is to compare the NDF for both the scenarios and see whether there is a common trend. MACOM has recently implemented the NDF analysis in some of their simpler non-linear models consisting of single control sources within the FET, however, further work is required to implement the NDF in their preferred more sophisticated non-linear Meerkat pHEMT model. The Meerkat model contains FETs that have multiple control sources and so this thesis work which looks into a double VCCS source model would help with the implementation process. Currently, it is difficult to determine whether the order in which the control sources are turned off for Return Ratio calculations play a role in the overall NDF analysis or not. Since, calculating the NDF based on the Return Ratio method only takes into account the products of the Return Ratio of each control source, the order should not matter and this is exactly what will be observed in this thesis.

### Scenario 1

Exciting the first control source, which is represented by the transconductance value  $g_{mA}$  through an external stimulus and using equation 3.1.

$$\begin{bmatrix} y_{11} & y_{12} & y_{13} & y_{14} & y_{15} \\ y_{21} + g_{mB} & y_{22} & y_{23} & y_{24} & y_{25} - g_{mB} \\ y_{31} & y_{32} & y_{33} & y_{34} & y_{35} \\ y_{41} - g_{mB} & y_{42} & y_{43} & y_{44} & y_{45} + g_{mB} \\ y_{51} & y_{52} & y_{53} & y_{54} & y_{55} \end{bmatrix} \times \begin{bmatrix} v_1 \\ v_2 \\ v_3 \\ v_4 \\ v_5 \end{bmatrix} = \begin{bmatrix} 0 \\ -g_{mA} \cdot v_{ext} \\ 0 \\ g_{mA} \cdot v_{ext} \\ 0 \end{bmatrix} \quad (3.2)$$

Exchanging the rows and columns, the terms with  $g_{mb}$  are collected together towards the top of the matrix, to be later used as a block matrix.

$$\begin{bmatrix} y_{21} + g_{mB} & y_{22} & y_{23} & y_{24} & y_{25} - g_{mB} \\ y_{41} - g_{mB} & y_{42} & y_{43} & y_{44} & y_{45} + g_{mB} \\ y_{11} & y_{12} & y_{13} & y_{14} & y_{15} \\ y_{31} & y_{32} & y_{33} & y_{34} & y_{35} \\ y_{51} & y_{52} & y_{53} & y_{54} & y_{55} \end{bmatrix} \times \begin{bmatrix} v_1 \\ v_2 \\ v_3 \\ v_4 \\ v_5 \end{bmatrix} = \begin{bmatrix} -g_{mA} \cdot v_{ext} \\ g_{mA} \cdot v_{ext} \\ 0 \\ 0 \\ 0 \end{bmatrix} \quad (3.3)$$

$$\begin{bmatrix} y_{21} + g_{mB} & y_{25} - g_{mB} & y_{22} & y_{23} & y_{24} \\ y_{41} - g_{mB} & y_{45} + g_{mB} & y_{42} & y_{43} & y_{44} \\ y_{11} & y_{15} & y_{12} & y_{13} & y_{14} \\ y_{31} & y_{35} & y_{32} & y_{33} & y_{34} \\ y_{51} & y_{55} & y_{52} & y_{53} & y_{54} \end{bmatrix} \times \begin{bmatrix} v_1 \\ v_5 \\ v_2 \\ v_3 \\ v_4 \end{bmatrix} = \begin{bmatrix} -g_{mA} \cdot v_{ext} \\ g_{mA} \cdot v_{ext} \\ 0 \\ 0 \\ 0 \end{bmatrix} \quad (3.4)$$

$$\begin{bmatrix} y_{21} + g_{mB} & y_{25} - g_{mB} \\ y_{41} - g_{mB} & y_{45} + g_{mB} \end{bmatrix} \times \begin{bmatrix} v_1 \\ v_5 \end{bmatrix} = \begin{bmatrix} -g_{mA} \cdot v_{ext} \\ g_{mA} \cdot v_{ext} \end{bmatrix} \quad (3.5)$$

After solving this  $2 \times 2$  matrix, the Return Ratio,  $RR_1$  is obtained. By solving a similar matrix equation but this time setting exciting the VCCS with transconductance  $g_{mB}$  and setting  $g_{mA}$  to zero, Return Ratio,  $RR_2$  is obtained. The two results are then used to calculate the NDF as follows.

$$\begin{aligned} NDF &= (RR_1 + 1)(RR_2 + 1) \\ &= \frac{g_{mA}A + g_{mB}B + C}{g_{mB}B + C} \times \frac{g_{mB}D + g_{mA}E + F}{g_{mA}E + F} \end{aligned}$$

where,

$$A = y_{41} + y_{21} + y_{45} + y_{25}$$

$$B = y_{21} + y_{45} - y_{41} - y_{25}$$

$$C = y_{21}y_{43} - y_{41}y_{25}$$

$$D = y_{41} + y_{21} + y_{43} + y_{23}$$

$$E = y_{21} + y_{43} - y_{41} - y_{23}$$

$$F = y_{21}y_{43} - y_{41}y_{23}$$

This was the first scenario calculation, where each of the current sources were excited successively and in the excitation of the second source, the first source was switched off to zero. The next step is to look at the scenario where both the current sources are probed by an external voltage source together.

## Scenario 2

The network matrix remains unchanged and is the same as equation 3.1, however, since both the sources are excited together, the resulting matrix for this scenario can be shown below.

$$\begin{bmatrix} y_{21} & y_{23} & y_{25} & y_{22} & y_{24} \\ y_{41} & y_{43} & y_{45} & y_{42} & y_{44} \\ y_{11} & y_{12} & y_{13} & y_{14} & y_{15} \\ y_{31} & y_{32} & y_{33} & y_{34} & y_{35} \\ y_{51} & y_{52} & y_{53} & y_{54} & y_{55} \end{bmatrix} \times \begin{bmatrix} v_1 \\ v_3 \\ v_5 \\ v_2 \\ v_4 \end{bmatrix} = \begin{bmatrix} -(g_{mA} + g_{mB}) \cdot v_{ext} \\ (g_{mA} + g_{mB}) \cdot v_{ext} \\ 0 \\ 0 \\ 0 \end{bmatrix} \quad (3.6)$$

$$\begin{bmatrix} y_{21} & y_{23} & y_{25} \\ y_{41} & y_{43} & y_{45} \\ y_{11} & y_{12} & y_{13} \end{bmatrix} \times \begin{bmatrix} v_1 \\ v_3 \\ v_5 \end{bmatrix} = \begin{bmatrix} -(g_{mA} + g_{mB}) \cdot v_{ext} \\ (g_{mA} + g_{mB}) \cdot v_{ext} \\ 0 \end{bmatrix} \quad (3.7)$$

Solving this  $3 \times 3$  matrix requires the knowledge of solving the inverse of a  $3 \times 3$  matrix which is learnt off from the Khan Academy tutorials [2].

The following NDF expression is obtained from the calculation.

$$NDF = \frac{[(g_{mA} + g_{mB})A + X] \times [(g_{mA} + g_{mB})B + X]}{X^2}$$

where,

$$A = y_{43}y_{13} - y_{12}y_{45} - y_{11}y_{45} + y_{41}y_{13} - y_{12}y_{25} + y_{23}y_{13} - y_{21}y_{13} + y_{11}y_{25}$$

$$B = -y_{41}y_{12} + y_{11}y_{43} + y_{11}y_{23} - y_{21}y_{12} + y_{43}y_{13} - y_{12}y_{45} - y_{12}y_{25} + y_{23}y_{13}$$

$$X = y_{21}(y_{43}y_{13} - y_{12}y_{45}) - y_{23}(y_{41}y_{13} - y_{11}y_{45}) + y_{25}(y_{41}y_{12} - y_{11}y_{43})$$

The results from both the analysis seems to be quite different and cannot be simplified to present a common solution. It can therefore not be concluded that the two current sources excited successively as Struble described in [10] is the same as exiting them together in one single step. The other thing to note is that the  $5 \times 5$  matrix makes the whole process much more tedious as there are too many admittance parameters to deal with.

### 3.1 Calculating NDF for a Single Three-Port FET Model

Since, the results from the five-port network calculations did not match as expected, the next logical step was to take a closer look at what happens when the behaviour of a simple single three-port network such that of a FET is observed. **The FET is represented in a small signal model with two dependent current sources that are equal in magnitude and opposite in direction.** The model used to represent the three port FET can be shown below in figure 3.2. We use a FET in this case as engineers at MACOM have already implemented the NDF in some of their models using FETs.

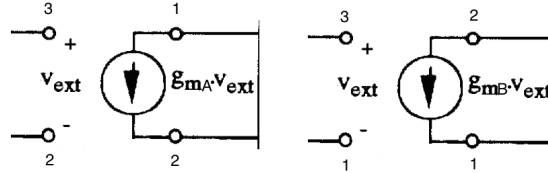


**Figure 3.2:** Three-Port FET model with an additional control source

The calculations are carried out in the same way, as explained in the two previous scenarios using equation 2.10

$$Y(S) * V(S) = I(S).$$

The admittance network can be represented in the equation below.

$$\begin{bmatrix} y_{11} - g_{mB} & y_{12} - g_{mA} & y_{13} + g_{mA} + g_{mB} \\ y_{21} + g_{mB} & y_{22} + g_{mA} & y_{23} - g_{mA} - g_{mB} \\ y_{31} & y_{32} & y_{33} \end{bmatrix} \times \begin{bmatrix} v_1 \\ v_2 \\ v_3 \end{bmatrix} = \begin{bmatrix} i_1 \\ i_2 \\ i_3 \end{bmatrix} \quad (3.8)$$

For, the first scenario, the two sources are excited one at a time. In this instance, the control source with transconductance,  $g_{mA}$  is excited by an external voltage source,  $V_{ext}$  and the other control source works normally. So, the following equation is obtained.

$$\begin{bmatrix} y_{11} - g_{mB} & y_{12} & y_{13} + g_{mB} \\ y_{21} + g_{mB} & y_{22} & y_{23} - g_{mB} \\ y_{31} & y_{32} & y_{33} \end{bmatrix} \times \begin{bmatrix} v_1 \\ v_2 \\ v_3 \end{bmatrix} = \begin{bmatrix} g_{mA} \cdot v_{ext} \\ -g_{mA} \cdot v_{ext} \\ 0 \end{bmatrix} \quad (3.9)$$

$$RR_1 = \frac{-v_{32}}{v_{ext}}$$

Exchanging columns and rows and using the concept of partitioned matrix [7], the following is obtained.

$$\begin{bmatrix} y_{12} & y_{13} + g_{mB} & y_{11} - g_{mB} \\ y_{22} & y_{23} - g_{mB} & y_{21} + g_{mB} \\ y_{32} & y_{33} & y_{31} \end{bmatrix} \times \begin{bmatrix} v_2 \\ v_3 \\ v_1 \end{bmatrix} = \begin{bmatrix} g_{mA} \cdot v_{ext} \\ -g_{mA} \cdot v_{ext} \\ 0 \end{bmatrix} \quad (3.10)$$

$$\begin{bmatrix} y_{12} & y_{13} + g_{mB} \\ y_{22} & y_{23} - g_{mB} \end{bmatrix} \times \begin{bmatrix} v_2 \\ v_3 \end{bmatrix} = \begin{bmatrix} g_{mA} \cdot v_{ext} \\ -g_{mA} \cdot v_{ext} \end{bmatrix} \quad (3.11)$$

By solving the above equation,  $RR_1$  is obtained as follows.

$$RR_1 = \frac{g_{mA}(y_{23} + y_{13} + y_{22} + y_{12})}{y_{12}(y_{23} - g_{mB}) - y_{22}(y_{13} + g_{mB})}$$

In the next step, the control source with transconductance  $g_{mB}$  is excited and the first control source is set to zero. The equation for this step is as follows.

$$\begin{bmatrix} y_{11} & y_{12} & y_{13} \\ y_{21} & y_{22} & y_{23} \\ y_{31} & y_{32} & y_{33} \end{bmatrix} \times \begin{bmatrix} v_1 \\ v_2 \\ v_3 \end{bmatrix} = \begin{bmatrix} g_{mB} \cdot v_{ext} \\ -g_{mB} \cdot v_{ext} \\ 0 \end{bmatrix} \quad (3.12)$$

The Return Ratio for this step,  $RR_2$  is obtained in the same way as before and the NDF is calculated as follows.

$$RR_2 = \frac{g_{mB}(y_{23} + y_{13} + y_{21} + y_{11})}{y_{11}y_{23} - y_{21}y_{13}}$$

$$NDF = (RR_1)(RR_2) = \frac{g_{mA}g_{mB}AB + g_{mA}AC + g_{mB}BD + DC}{DC}$$

where,

$$A = y_{23} + y_{13} + y_{22} + y_{12}$$

$$B = y_{23} + y_{13} + y_{21} + y_{11}$$

$$C = y_{11}y_{23} - y_{21}y_{13}$$

$$D = y_{21}y_{23} - y_{12}g_{mB} - y_{22}y_{13} - y_{22}g_{mB}$$

Moving on from the results that have been obtained by subsequent excitation and switching of the control sources, we now look at the Scenario 2 where both the VCCS are excited together. These calculations are still based on the model shown in figure 3.2 and the equation still remains the same as equation 3.8.

In order to observe what happens when both the sources are excited together, the following equation is derived.

$$\begin{bmatrix} y_{11} & y_{12} & y_{13} \\ y_{21} & y_{22} & y_{23} \\ y_{31} & y_{32} & y_{33} \end{bmatrix} \times \begin{bmatrix} v_1 \\ v_2 \\ v_3 \end{bmatrix} = \begin{bmatrix} (-g_{mA} + g_{mB}) \cdot v_{ext} \\ (g_{mA} - g_{mB}) \cdot v_{ext} \\ 0 \end{bmatrix} \quad (3.13)$$

This  $3 \times 3$  will have to be solved to obtain the NDF. The final result is as follows

$$NDF = \frac{(g_{mA}^2 + g_{mB}^2)(AB) - 2ABg_{mA}g_{mB} + (g_{mA} - g_{mB})(AX + BX) + X^2}{X^2}$$

where,

$$A = -y_{22}y_{33} + y_{32}y_{23} - y_{31}y_{12} + y_{11}y_{32} + y_{32}y_{13} - y_{12}y_{33} + y_{21}y_{32} - y_{31}y_{22}$$

$$B = -y_{31}(y_{23} + y_{13} + y_{22} + y_{12}) + y_{33}(y_{21} + y_{11}) + y_{32}(y_{22} + y_{11})$$

$$X = y_{22}(y_{11}y_{33} - y_{13}y_{31}) + y_{12}(y_{23}y_{31} - y_{21}y_{33}) + y_{32}(y_{13}y_{21} - y_{11}y_{23})$$

It can be observed, that the NDF results for when both the VCCS are controlled successively and when they are switched simultaneously, are quite different algebraically. In order to understand this phenomenon a bit better, we take a closer look at the implementation being carried out in the Microwave Office AWR circuit simulator which is discussed in greater details in chapter 4.

## Chapter 4

# Small Signal Implementation in circuit simulator AWR

Since, we have not been able to conclude a great deal from the mathematical analysis of the three port FET model, we now look at the small signal implementation to compare results from the two switching patterns. In order to do this, the current model provided by Bryan Schwitter from MACOM that uses single control source FETs will need to be modified to include a second control source. Before the small signal implementation could be carried out, the existing model has to be verified to see if it is working properly as expected. It would be unwise to employ the second control source when it has not been ensured that the circuit model provided by MACOM is working perfectly fine.

Following figure 4.1 is the AWR model provided by MACOM

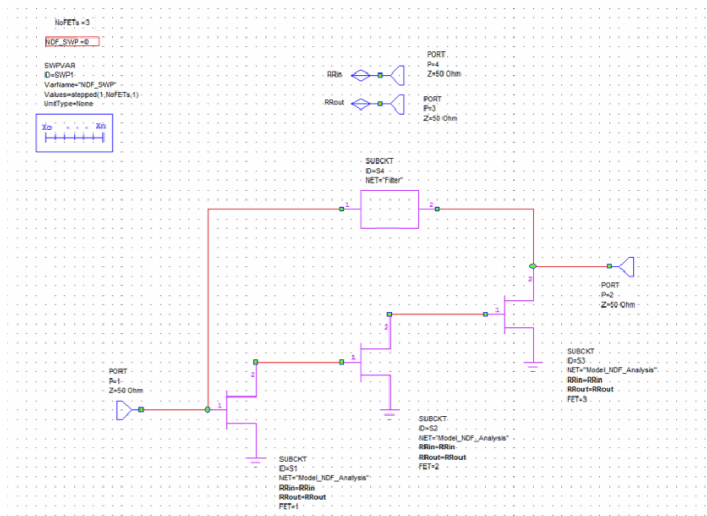


Figure 4.1: Top Level Circuit model diagram in AWR (obtained from MACOM)

When we go into the second and third bottom level of this circuit we obtain the following figure 4.2 and figure 4.3.

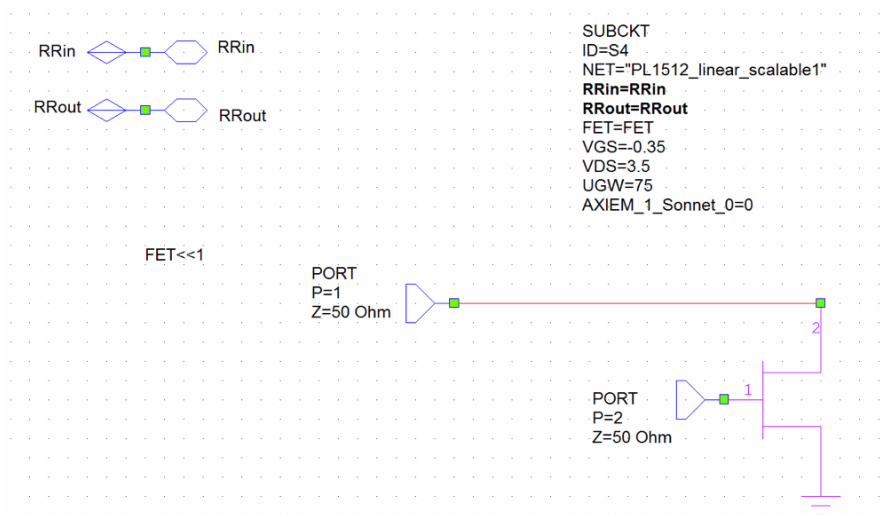


Figure 4.2: Second Level Circuit model diagram in AWR

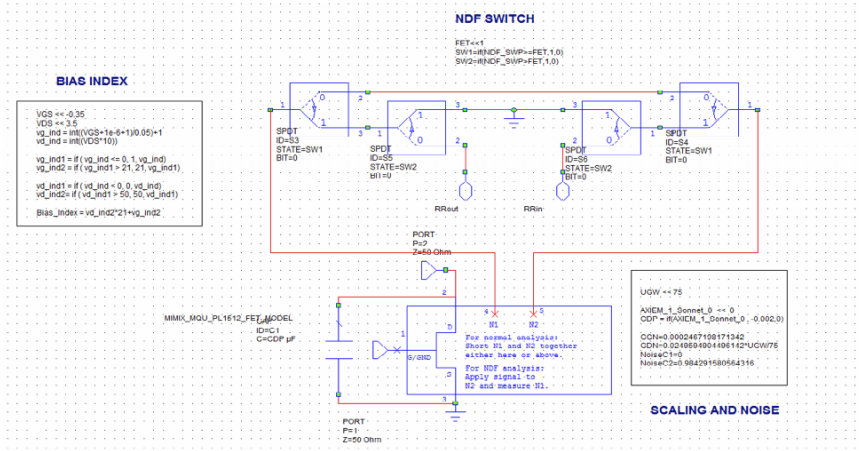


Figure 4.3: Bottom Level Circuit model diagram in AWR

The following figure 4.4 is the LRC filter circuit which is represented as sub circuit in the top level AWR circuit model in figure 4.1. This LRC circuit consists of an inductor (L), a resistor (R) and a capacitor (C), connected in series.

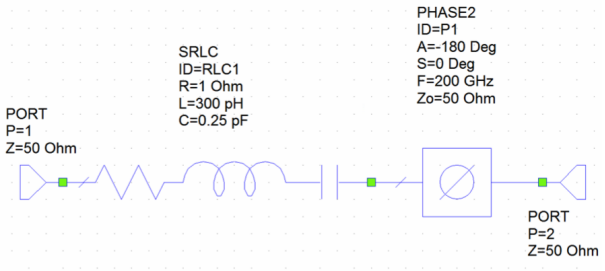
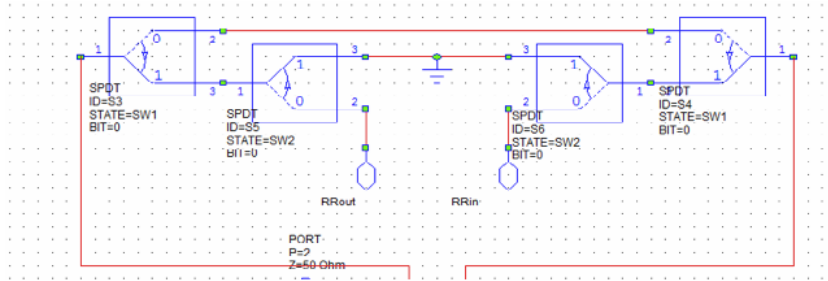


Figure 4.4: Filter circuit as shown in the top Level of AWR circuit model

Since, two transistors are used, there is the need for a switching block to control the switching pattern of the two transistors. The calculation of Return Ratio requires subsequent switching on and off of the two transistors. The switching block is included within each FET and can be shown in figure 4.5.



**Figure 4.5:** Switching block included within the individual FET

## 4.1 Modification of the existing circuit model

The model provided from MACOM was looked at thoroughly and some corrections needed to be made in the output equations. With the current model provided by MACOM, the NDF calculations did not seem to work properly. This was checked by simplifying the model to work with a single transistor first. The single transistor model was used to calculate the Return Ratio and then that value of Return Ratio was used to calculate the NDF. Meanwhile an experimental NDF was also calculated using the equations provided by the MACOM Engineers. It was found that there were some discrepancies between the two. The NDF equation was measured from the same circuit. The equations are given as follows.

$$NDF_{34} = NDF_{TEST\_EXAMPLE} : S(3, 4) \quad (4.1)$$

$$RR = -NDF_{S34}/2 \quad (4.2)$$

$$NDF = (RR^{[*], 1} + 1) * (RR^{[*], 2} + 1) * (RR^{[*], 3} + 1) \quad (4.3)$$

$$NDF_{encirclements} = unwrap(angle(NDF), _PI)/(-2 * _PI) \quad (4.4)$$

Both the equations and the model had to be changed for the NDF calculation to work properly. The following are the changes that were made to the model.

1. The first change was to ensure that only a single transistor was in operation. To do this, the two other transistors had to be disabled and the number of transistors had to be changed to 1 to avoid sweeping, since there is no sweeping required.
2. The  $RR_{out}$  port impedance as shown in figure 4.1 was causing the results to differ as the port impedance of 50 ohm resistor was adding to the overall circuit impedance. In order to neglect the effect of this port impedance, the impedance was increased to the order of  $1 \times 10^6$  ohm.
3. The top level port impedances also hampered the circuit impedance hence was grounded using resistors. Simple grounding resulted in an error in AWR, so a 1 Ohm resistor was used.
4. Changes in the LRC filter circuit
  - (a) If we look at the LRC filter circuit as shown in figure 4.4, we will see that a phase shifter has been used. The phase shifter is only required when more than two transistors are used. For this purpose, we also disabled the phase shifter.

- (b) Previously, the complex value of impedance,  $Z$ , of the filter circuit was read off as a sub circuit however, it was found that to realise the actual complex value of the LRC circuit impedance, it was required to measure the impedance,  $Z$ , in isolation of the rest of the circuit by measuring the impedance against one port and grounding the other.

## Single FET

After the above changes and simplifications had been made to the circuit model the new Return Ratio was calculated. The modified circuit model can be shown in figure 4.6 and figure 4.7. This calculation of the Return Ratio is done in the method described in Chapter 3 where the Y, admittance matrix of the transistor model has to be obtained first.

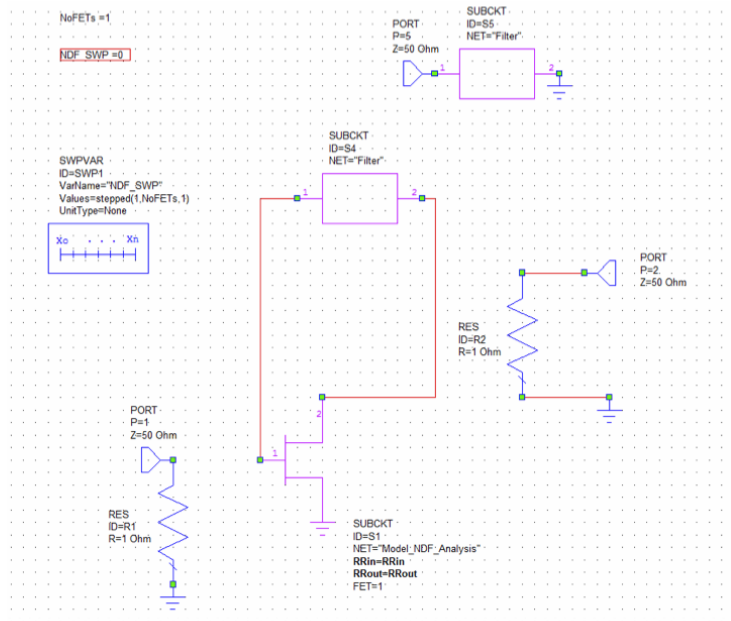
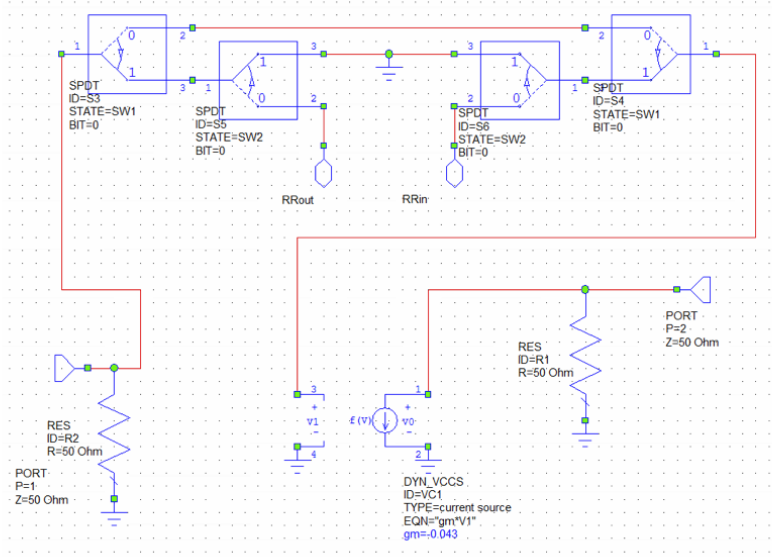


Figure 4.6: Modified circuit model



**Figure 4.7:** Modified circuit model

The admittance matrix of the model shown in figure 4.6 is obtained as shown below.

$$\begin{bmatrix} Y + Y_I & -Y \\ -Y + g_m & Y + Y_L \end{bmatrix} \times \begin{bmatrix} v_1 \\ v_2 \end{bmatrix} = \begin{bmatrix} i_1 \\ i_2 \end{bmatrix} \quad (4.5)$$

By probing the control source having transconductance  $g_m$  with an external source, the following is obtained.

$$\begin{bmatrix} Y + Y_I & -Y \\ -Y & Y + Y_L \end{bmatrix} \times \begin{bmatrix} v_1 \\ v_2 \end{bmatrix} = \begin{bmatrix} 0 \\ -g_m v_{ext} \end{bmatrix} \quad (4.6)$$

From the above matrix shown in equation 4.6, the following simplifications were made

$$(Y + Y_I)v_1 - Yv_2 = 0$$

$$-Yv_1 + (Y + Y_L)v_2 = -g_m v_{ext}.$$

Solving these two equations, the Return Ratio and the NDF can be calculated as follows.

$$RR = -\frac{v_I}{v_{ext}} = \frac{-g_m Y}{(Y + Y_L)(Y + Y_I) - Y^2}.$$

Assuming,  $g_m = -1$  and  $Z_L = Z_I = 50$ , the following is obtained

$$RR = \frac{Y}{(Y + \frac{1}{50})(Y + \frac{1}{50}) - Y^2}.$$

Next, the whole equation is expressed in terms of impedance,  $Z$

$$RR = \frac{Z}{(1 + \frac{Z^2}{50}) - 1}.$$

Hence,

$$NDF = RR + 1 = \frac{Z}{(1 + \frac{Z^2}{50}) - 1} + 1. \quad (4.7)$$

The above equation 4.7 was used to measure the NDF value and compare it to the quantity measured. The point to be noted here is that the equation 4.7 is calculated using the transconductance value,  $g_m$  to be negative unity so it is expected the NDF measurement and the calculations will only match and overlap when  $g_m$  is -1. NDF is a complex quantity so it is necessary to analyse both the magnitude and the angle plots separately. The results obtained are as follows.

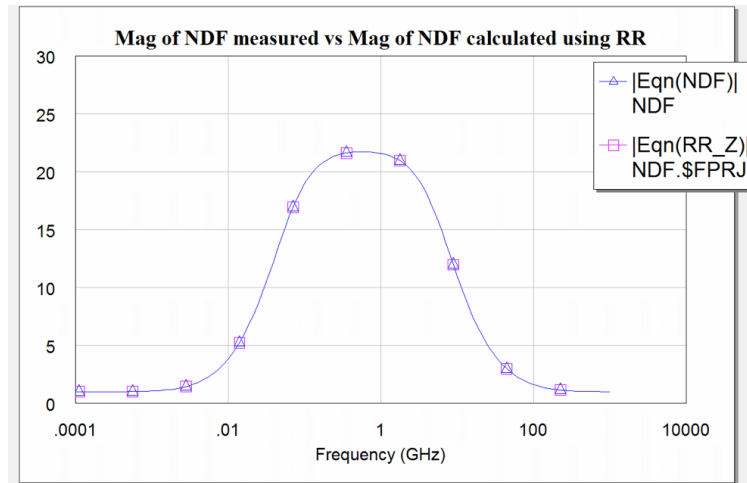


**Figure 4.8:** Magnitude of NDF versus Magnitude of NDF calculated using equation 4.7

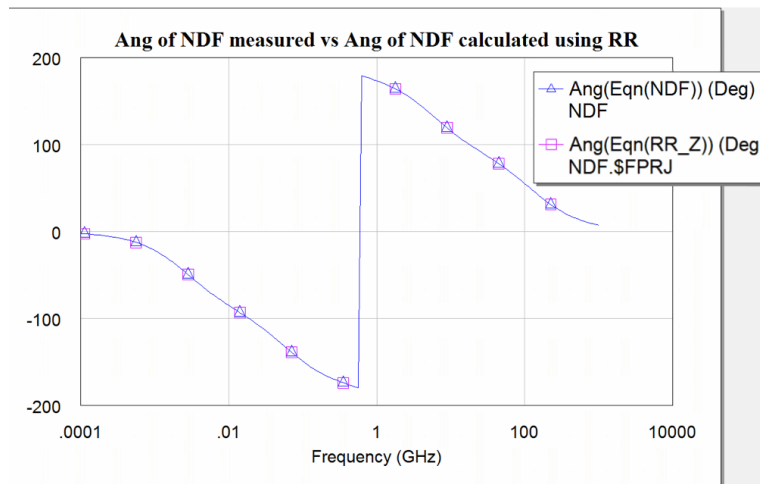


**Figure 4.9:** Angle of NDF versus Angle of NDF calculated using equation 4.7

It can be observed in figure 4.8 and figure 4.9 that the two plots, one of NDF measurement and the other of NDF calculation are perfectly overlapping on each other, which proves that the NDF measurement from the new modified circuit model is working correctly. The encirclements of the complex quantity of NDF can be represented in the form of a trajectory swept over an angular frequency,  $\omega$  of  $-\infty$  to  $+\infty$  which can be shown as in figure 4.10.

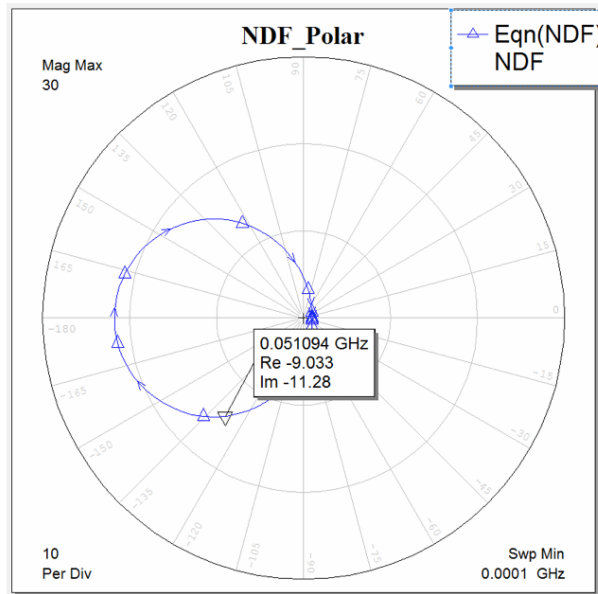


**Figure 4.10:** NDF Encirclements around the origin representing zeroes on the RHP

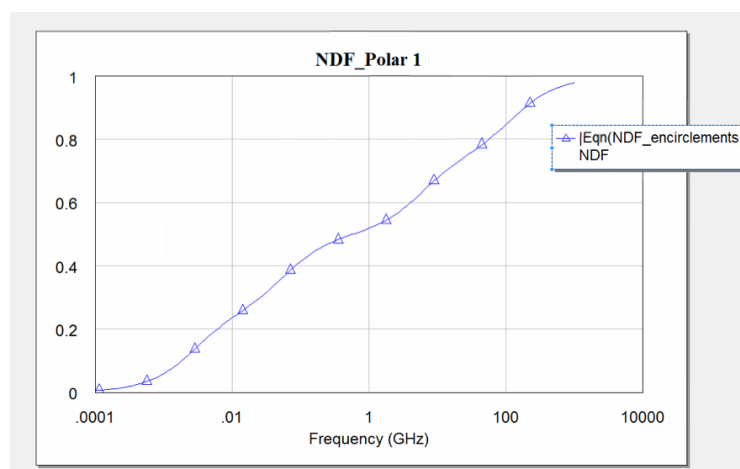


**Figure 4.11:** The number of encirclements around the origin

The figure 4.11 represents the number of encirclements of the Normalised Determinant Function around the origin. It can be seen that it has not quite reached the 1 mark yet meaning the circuit is still stable. So, in order to increase the number of encirclements and observe the instability behaviour, the transconductance,  $g_m$  has to be changed. The results are discussed in the following chapter.



The number of encirclements i.e zeroes on the RHP can be increased in a number of ways. One way of increasing the number of zeroes is by introducing a second filter (LRC) circuit in the circuit model. A single LRC circuit can only provide a **single encirclement of  $180^\circ$  from  $-90^\circ$  to  $+90^\circ$  degree** whereas two FETs produce two encirclements of  $180^\circ$  each. This can be represented in figure 4.13

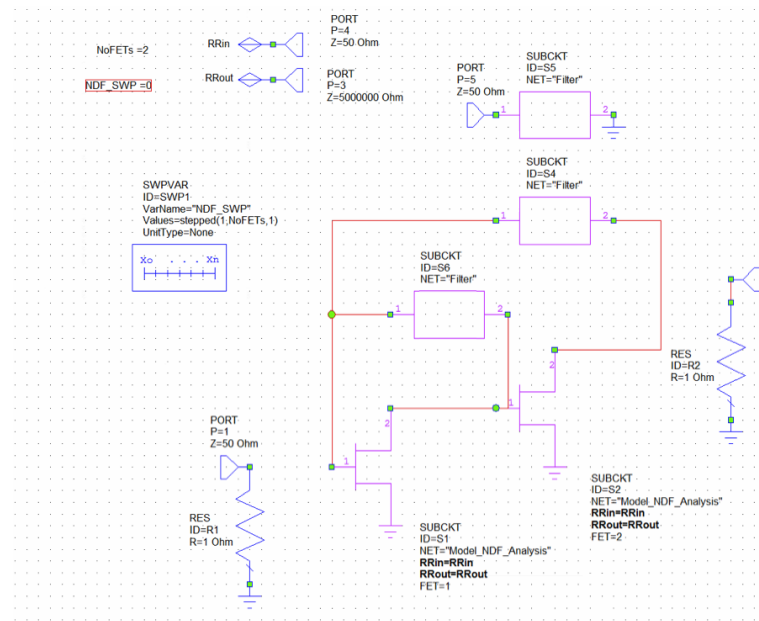


**Figure 4.13:** The modified circuit model to include a second LRC filter circuit

This can be observed when the value of transconductance,  $g_m$  is tuned to see two clear encirclements on both the polar trajectory and the encirclement plot. This can be shown in figure 4.14 and figure 4.15.

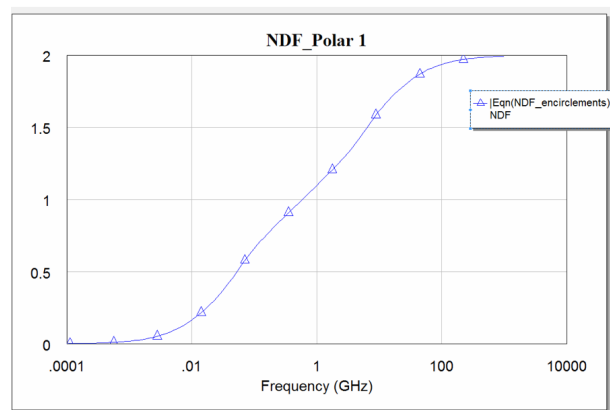
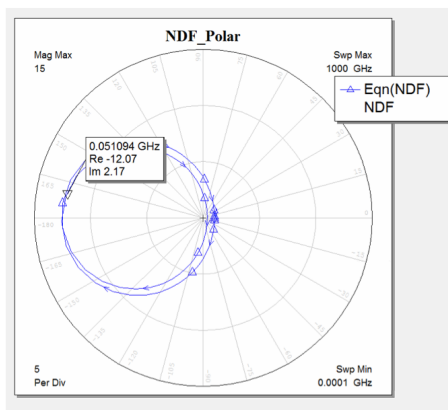


**Figure 4.14:** NDF Encirclement trajectory on a polar plot when  $g_m = 0.12$

**Figure 4.15:** Number of encirclements and zeroes on the RHP when  $g_m = 0.12$

## 4.2 Implementation of the two control sources in the switching model

The next step in the thesis is to implement the two control sources within the modified Two FET model as described in the previous section. A part of the solution to the bigger problem of providing a general solution to arbitrary circuits and implementing the NDF stability analysis in the Meerkat pHEMT problem is to observe and compare the result of when there are multiple control sources within a transistor and what the Return Ratio calculation algorithm looks like.

To observe this behaviour, this thesis looks at different switching models for when there are two control sources. It is assumed that the NDF calculation carried out by the subsequent excitation and switching of the two control sources yield similar results to when the two control sources are excited together. This is because the NDF calculation depends on the products of the Return Ratios so the order in which the excitation and switching occurs should not matter. This will be proven through this part of the experiment.

The two different switching models are shown below in figure 4.16 and figure 4.17.

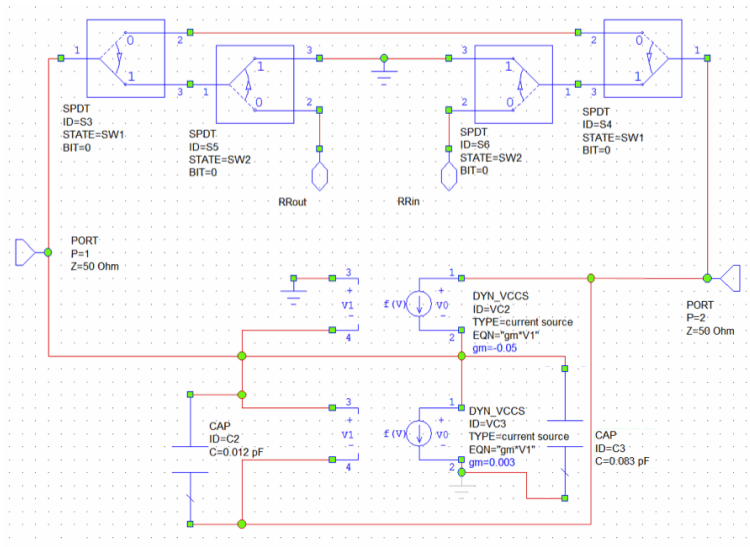


**Figure 4.16:** Two FET two control source FET model with a shared switching block

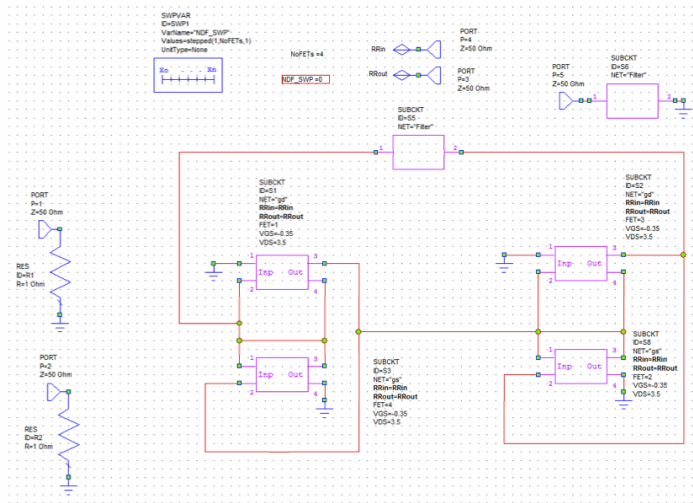


Figure 4.17: Two FET two control source model with individual switching blocks

In the first model represented by figure 4.16, it can be observed that there is only one switching network for both the sources which means that the two control sources get excited together and the NDF measurement is carried out. This circuit model follows the same hierarchical structure as the model provided by MACOM where at the top level, two FETs can be seen and at the bottom most level, the control sources can be seen.

On the contrary, figure 4.17 represents a new hierarchical model where on the top level, the two FETs can be observed in terms of the two control sources. The two control sources are denoted by two black boxes for each FET, totalling to 4 control sources altogether. The two control source model each have their own switching network and this can be observed when looked at the bottom most hierarchy level. Each control source is represented using a black box so going into the subcircuit, the gate-drain and the gate-source connections of the FET can be seen. This can be shown in figure 4.18 and figure 4.19.

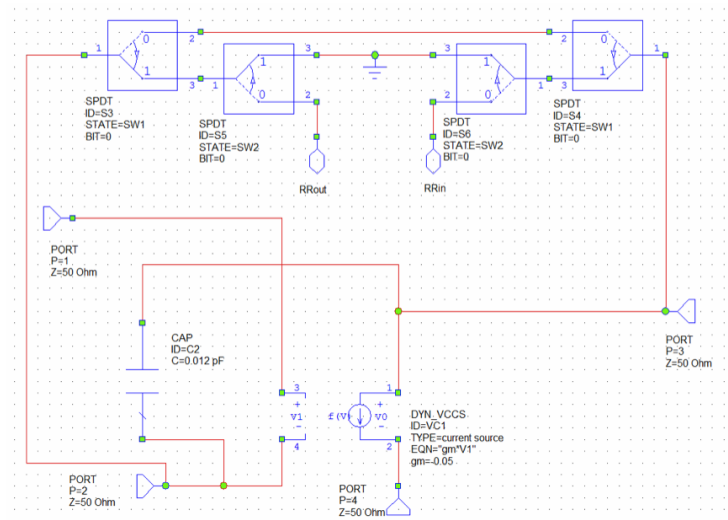


Figure 4.18: Control source with gate-drain connections

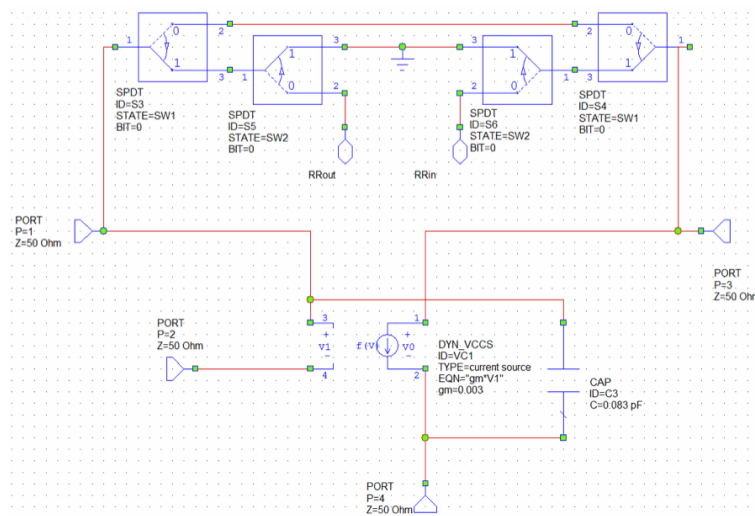


Figure 4.19: Control source with gate-source connections

The values used to define the transconductances,  $g_m$  on each gate-drain and gate-source connections and the capacitance values are that of a linear FET model obtained from MACOM by S parameter measurements of a pHEMT. It describes the behaviour of the intrinsic device channel i.e. how the semiconductor behaves, separated from the devices metalisation. The values are measured over a frequency range of 50MHz to 50 GHz but do not vary much with frequency. The values used are that of frequency 10 GHz.

The results obtained from these circuit models will be analysed and compared in chapter 5.

# Chapter 5

## Comparison of analysis approach

It is important to understand the different circuit models used in this thesis to draw up a comparison analysis. This comparison analysis will help understand the underlying differences in adding additional FETs and voltage controlled current sources and how it affects the polar trajectory and encirclement plots and hence the stability of the circuit as shown in figure 4.10 and figure 4.11. The models used are defined as follows.

1. Single FET model with single control source
2. Two FET model with single control source
3. Two FET model with double control source
  - (a) Double control source model controlled and excited together (one shared switching network)
  - (b) Double control source model with individual switching network

The results, i.e. the polar trajectory plot and the encirclement plot by sweeping  $\omega$  from 0 to  $-\infty$  from both the single and double FET model each with single control sources can be compared to see if there are any similarities or notable differences in the number of zeroes on the RHP and stability.

### 5.1 Results for Single FET single source

The following are graphs of varying transconductance,  $g_m$  values of the voltage controlled current source. These graphs represent values  $g_m = -0.05$  and  $g_m = 0.042$ .

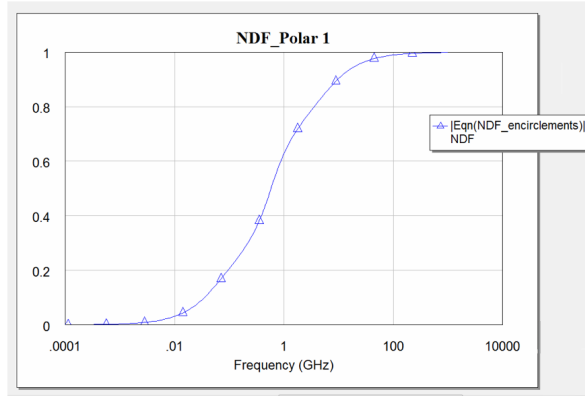
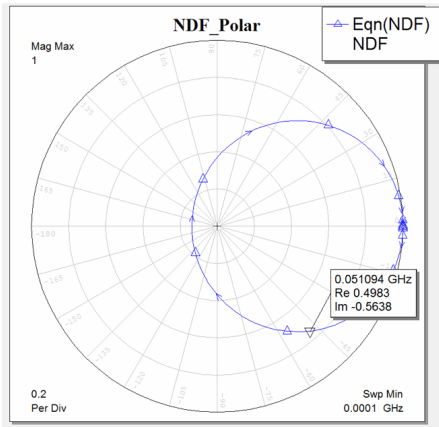


**Figure 5.1:** NDF Encirclement trajectory on a polar plot when  $g_m = -0.05$  **Figure 5.2:** Number of encirclements when  $g_m = -0.05$

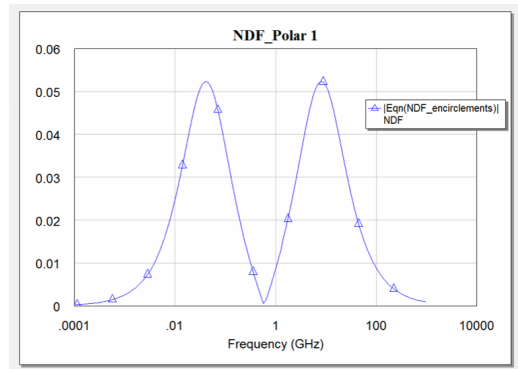
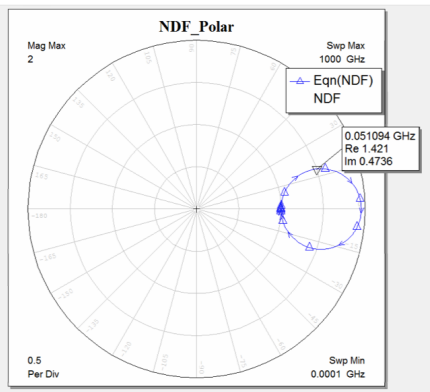


**Figure 5.3:** NDF Encirclement trajectory on a polar plot when  $g_m = 0.042$  **Figure 5.4:** Number of encirclements when  $g_m = 0.042$

## 5.2 Results for Two FETs single source

Now, the behaviour of the Two FET model can be observed using the same values of transconductance,  $g_m$  as used for the single FET model. The following represents graphs when  $g_m = -0.05$  and  $g_m = 0.042$ . These values were chosen with the use of a tuning tool to display clear encirclement plots.

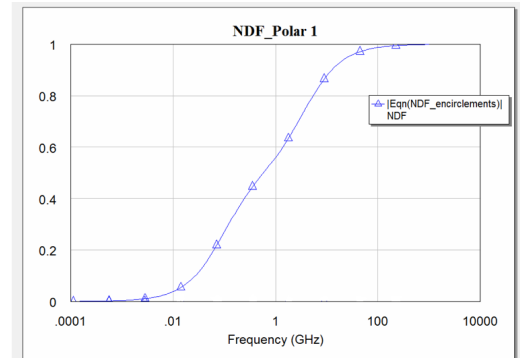
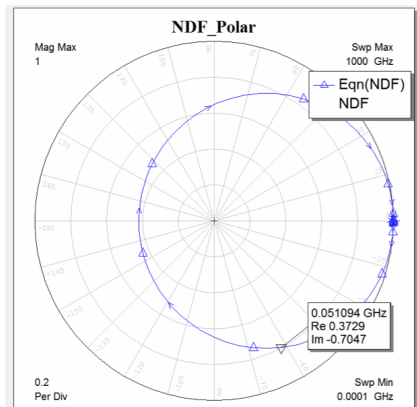


**Figure 5.5:** NDF Encirclement trajectory on a polar plot when  $g_m = -0.05$

**Figure 5.6:** Number of encirclements when  $g_m = -0.05$

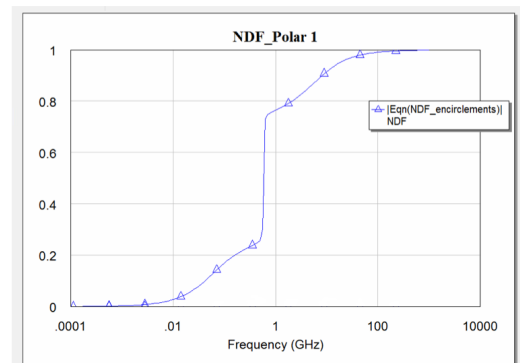
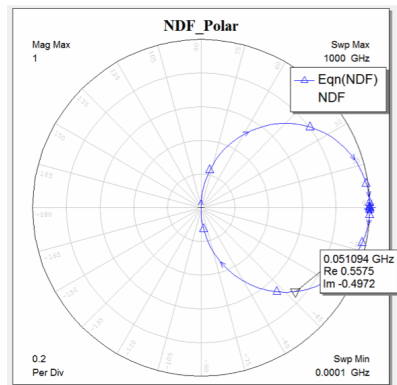


**Figure 5.7:** NDF Encirclement trajectory on a polar plot when  $g_m = 0.042$

**Figure 5.8:** Number of encirclements when  $g_m = 0.042$

With the help of a tuning tool in AWR, it is observed in the case of a single FET, the lower the transconductance value, below  $-0.05$ , the higher the encirclements, i.e the zeroes on the RHP starting from one. At a value greater than  $-0.05$ , a single FET has no encirclement. A clear encirclement can only be observed when the value of  $g_m < -0.05$ .

With the aid of the same tuning tool, it is observed that using two FETs the polar trajectory is slightly different. One encirclement is achieved by the Two FET model when the transconductance value is when  $-0.09 < g_m < -0.05$ , making the model unstable only in that range of  $g_m$ .

## 5.3 Results for Two FET, Two Control Source Model

This section can be divided to look into the two different models.

### Double control source model containing a single switching network

This particular model makes use of two FETs, each having two VCCS that share a single switching network. This switching network is used to excite the two FETs simultaneously. The aim of the thesis is to look at the concept of multiple control sources as a novel area of research and provide with mathematical and practical evidence to confirm that the order in which the control sources are excited and the Return Ratios calculated have no effect on the final NDF calculation and stability. It is expected that the model with a shared switching network will yield a similar result to when the sources are controlled individually. The first model developed as represented in figure 4.16 produces the following encirclement graphs. The output equations to get to these results are very similar to the equation 4.1, 4.2, 4.3 and 4.4 and had to be modified slightly to reflect the number of FETs to achieve the encirclement plots shown in figure 5.9 and figure 5.10.

This method allows for the Return Ratios and in turn the NDF to be calculated in one single step by providing an external stimulus to both the sources at the same time, instead of calculating it in two successive steps as is in the case of using individual switching networks for the control sources.

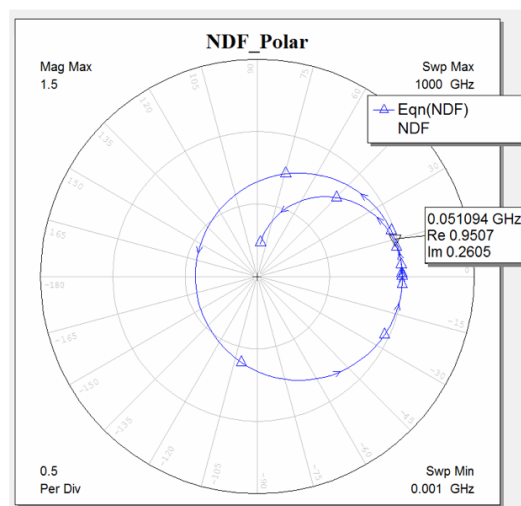


**Figure 5.9:** Polar trajectory plot by sweeping  $\omega$  from 0 to  $-\infty$

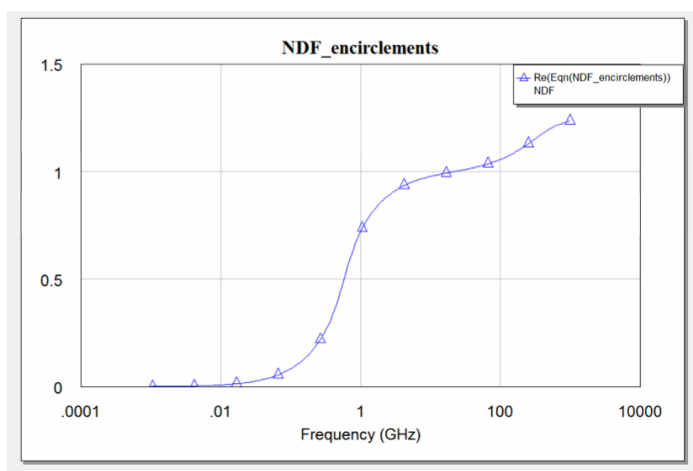
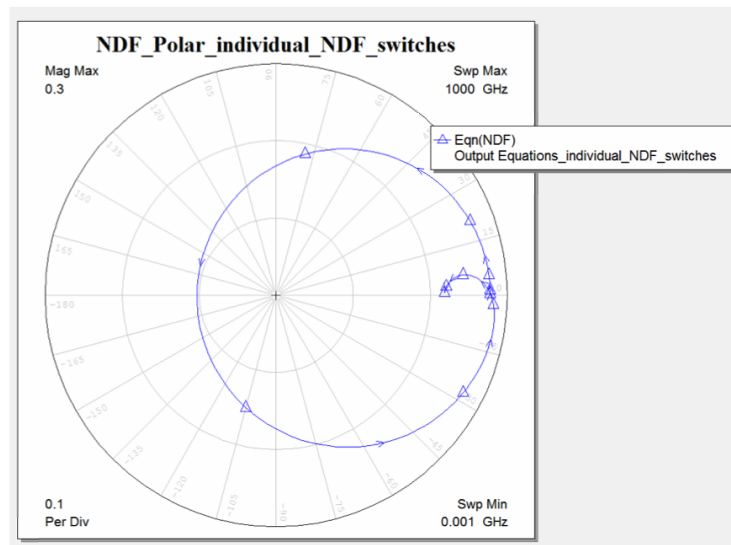


Figure 5.10: NDF encirclement plot by sweeping  $\omega$  from 0 to  $-\infty$

### Double control source model with individual switching network

The circuit model used to realise the individual switching network is represented in figure 4.17. This model allows for successive excitation and switching of the control sources. **In short, the two control sources are individually controlled and the NDF obtained using this model is calculated in two steps through working out the Return Ratio. The first Return Ratio is obtained by providing an external stimulus to one source and allowing the other to work normally. And in the next step, the second source is excited with the first source switched off.**

The following are the NDF analysis graphs obtained for the above described model.



**Figure 5.11:** Polar trajectory plot by sweeping  $\omega$  from 0 to  $-\infty$

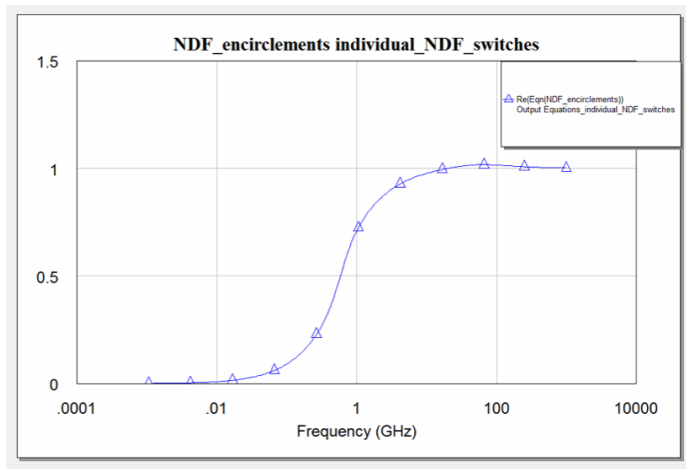


**Figure 5.12:** NDF encirclement plot by sweeping  $\omega$  from 0 to  $-\infty$

If the results from the two models are compared we can see that both produce very similar results. The NDF polar trajectory obtained by sweeping  $\omega$  from 0 to  $-\infty$  is slightly different for the two models but the number of encirclements and hence the number of zeroes in RHP obtained is the exact same since encirclements are only counted in whole numbers.

Thus, it can be concluded that the NDF analysis results obtained for any two control sources are the same whether the NDF measurement is carried out by subsequent excitation of the control sources or whether it is simultaneously probed with an external stimulus. This information is vital for determining the stability of any network containing multiple control sources.

## 5.4 Further Three FET model implementation

This thesis could be extended to a three FET model to match the initial model obtained from MACOM. Since, the foundation has already been established previously, this implementation is quite straightforward. A single FET is added to the existing model and the output equations for the NDF analysis has to be modified a bit to take into account the third FET. The following figure 5.13 represents the model.

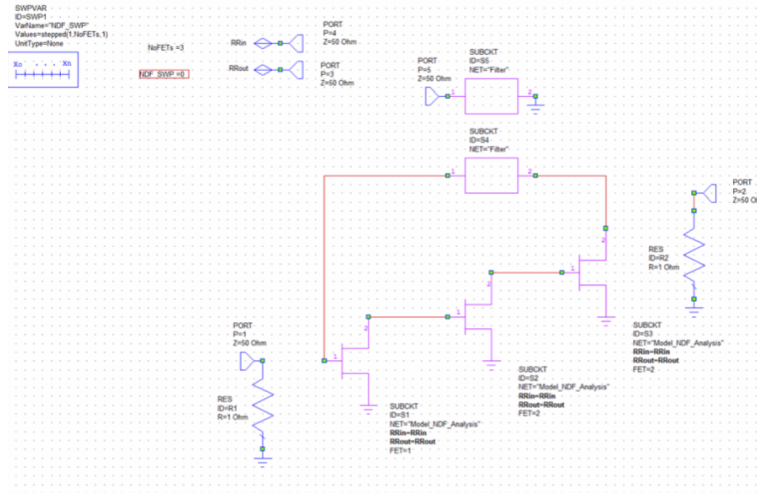


Figure 5.13: Three FET model for NDF analysis

Next, the NDF analysis can be carried out on this model and the NDF polar trajectory and the encirclement plots observed. The following figure 5.14 and figure 5.15 represents this NDF analysis plots.

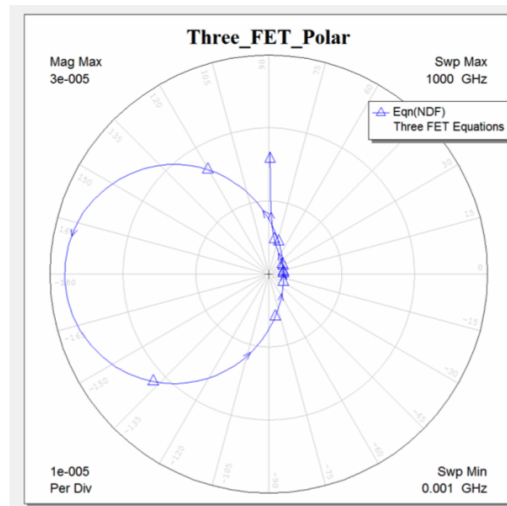
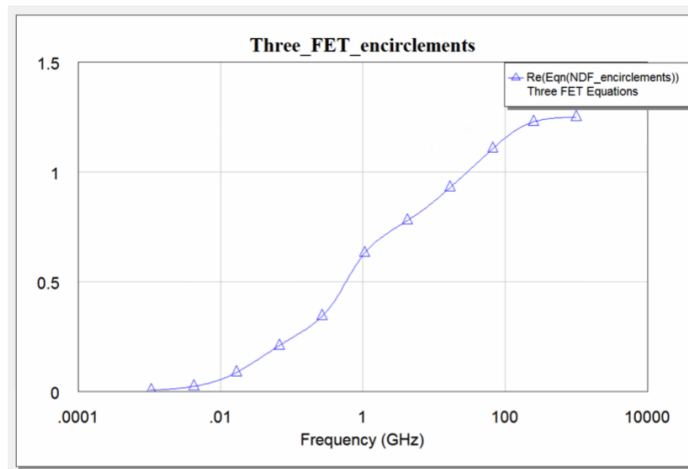


Figure 5.14: NDF polar trajectory plot by sweeping  $\omega$  from 0 to  $-\infty$



**Figure 5.15:** NDF encirclement plot by sweeping  $\omega$  from 0 to  $-\infty$

It can be observed that a three FET model yields a very similar result to a single FET and Two-FET model. Adding additional FETs to the model does not seem to vary the results greatly.

# Chapter 6

## Conclusion

This thesis is focussed on a very specialised area of interest for Macquarie University's industry partner MACOM Technology Solutions. For decades design engineers have relied on using the Linvill and Rollett (B and K) stability criteria to ensure stability of their circuits, however, both the B and K criteria have limitations. Recently, Struble [11] started working on a robust stability test called Normalised Determinant Function. Struble's work provided the foundation for this thesis however, this thesis was tailored to suit the implementation needs of MACOM.

MACOM have recently applied NDF in some simple linear models, however, some problems remain with the implementation of this useful feature in the more sophisticated and preferred non-linear model, Meerkat pHEMT model. One of the problems that arises with the implementation of the NDF in the Meerkat pHEMT model is that the model consists of multiple control sources in one single pHEMT and the study by Struble only looks at single control source transistors. This thesis is an extension to Struble's work and looks further into what the implications are in having multiple control sources and how it changes the NDF algorithm both algebraically and practically.

At the end of the thesis, it can be concluded that there is mathematical and practical evidence to prove that NDF can be implemented in the Meerkat PHEMPT model where each pHEMT has multiple control sources. This thesis will provide the foundation to implementing the NDF in arbitrary circuits and providing an overall solution to implement the NDF as a circuit stability test.

### Future Recommendations

It is recommended that the work in this thesis is carried to the next step in developing an overall solution to implementing the Normalised Determinant Function as an integral circuit stability test within the design process of amplifiers, etc. This can be achieved by looking at more realistic transistor models that are part of a bigger and more complex network containing lumped elements. The NDF algorithm will then have to be observed and analysed as to how realistic transistors behave and interact with other circuit elements. It is also necessary to extend this work to represent the number of control sources

within the Meerkat pHEMT model that is of interest to MACOM. This thesis only looks into the case of having two dependent sources within each FET whereas, the Meerkat model uses multiple sources. The results yielded from the different switching patterns of the sources will also have to be observed and taken into consideration when developing the overall general circuit stability.

# Chapter 7

## Abbreviations

NDF	Normalised Determinant Function
RHP	Right Hand Plane
FET	Field Effect Transistor
pHEMT	pseudomorphic High Electron Mobility Transistor
PDK	Process Design Kit
VCCS	Voltage Controlled Current Source



# Appendix A

## Project Attendance Form

This appendix contains the consultation meetings attendance form as required by the department. Both the supervisor and the student had to sign off the consultation meetings form for the official record of the meetings.

### Consultation Meetings Attendance Form

Week	Date	Comments (if applicable)	Student's Signature	Supervisor's Signature
Wk0	23/02/16	Meeting to discuss about the thesis	Sumiya	ARL
Wk1	29/02/16	Laying out the scope of the thesis	Sumiya	ARL
Wk2	07/03/16	Brushing up on background	Sumiya	ARL
Wk3	15/03/16	Discussing about the topic	Sumiya	ARL
Wk4	22/03/16	Checking the mathematical analysis	Sumiya	ARL
Wk5	29/03/16	Constraining the model to a FET with 3 nodes	Sumiya	ARL
Wk6	5/04/16	Small signal model discussion	Sumiya	ARL
Wk7	27/04/16	AWR Simulation Small signal implementation	Sumiya	ARL
Wk8	06/05/16	Small signal implementation	Sumiya	ARL
Wk10	17/05/16	Double source small signal model	Sumiya	ARL
Wk11	27/05/16	Meeting at MCOM Testing the switching model	Sumiya	
Wk12	02/06/16	Final meeting	Sumiya	



# Appendix B

## Related Paper

### A Rigorous Yet Simple Method For Determining Stability of Linear N-Port Networks

Wayne Struble and Aryeh Platzker

Raytheon Research Division  
131 Spring Street, Lexington, Massachusetts 02173

**Abstract** - Most GaAs MMIC designers use the well-known Linvill or Rollett [1-3] stability criteria (C or K) to *determine the stability* of linear two-port networks. These criteria have misled the circuit design community in that *they only apply to linear two-port networks that are stable to begin with*. In a paper by Platzker et al. [4], it was shown that these criteria are not rigorous because they only apply to linear networks with no poles in the right half plane (RHP). *Thus a separate test is required to determine if the network contains any poles in the RHP before the Linvill or Rollett stability criteria can be applied*. Platzker [4] describes a mathematically rigorous test based on contour plotting of a normalized determinant function for ascertaining the stability of linear networks. The intent of this paper is to describe a technique for easily calculating this determinant function using Return Ratios. It will be shown that an elegant yet simple relationship exists between the Return Ratios of each dependent source in a linear network and Platzker's normalized determinant function. Using this relationship, the stability (or instability) of linear N-port networks containing any number of active devices can easily be determined using commercially available circuit simulators. An example will be shown where this new technique correctly predicts instability in a GaAs MMIC power amplifier.

RHP, including the frequency axis  $\omega$ , the network will be unstable, otherwise the network is stable.

To most simply calculate the NDF, one can eliminate a number of nodes in the network by reducing it to a parallel connection of a passive and an active m-nodes where, depending on the nature of the dependent sources, m can be as large as four times and as small as twice the number of dependent sources. The network cannot be reduced further than this due to the possibility of introducing zeroes in the RHP of  $\Delta_{QN}$ . This can result in pole-zero cancellation in the NDF, and thus its locus may not encircle the origin (0,0) even when  $\Delta$  contains zeroes in the RHP.

In networks with more than five dependent sources, direct calculation of the NDF becomes difficult using commercially available circuit simulators. This is due to the limitation in the sizes of matrices that can be saved by the simulators for external calculations. LIBRA<sup>TM</sup>, for example, can save up to 20 port S parameter matrices. Calculation of the NDF inside the circuit simulator program is desirable since it allows stability sensitivity analysis or optimization of the network. To this end, we have derived an alternative way of easily calculating the NDF within the simulator using the concept of Return Ratios.

#### INTRODUCTION

Platzker's [4] normalized determinant function (NDF) is shown below:

$$\text{NDF} = \frac{\Delta}{\Delta_{QN}} \quad (1)$$

where  $\Delta$  represents the full network determinant (including all port terminations) and  $\Delta_{QN}$  represents the resulting passive network determinant when all N dependent sources (i.e. voltage controlled or current controlled sources) are set equal to zero. This is similar to Bode's [5] definition of the Return Difference  $\Delta / \Delta_0$  for a single dependent source, where  $\Delta_0$  represents the network determinant when the dependent source is set to zero. Note that any linear network parameters such as Y, Z, H etc. can be used to calculate the above determinants.

To determine stability, one would calculate the complex quantity NDF of a given network along the frequency axis  $\omega$  from  $+\infty$  to  $-\infty$  and plot its locus in the complex plane. If the locus of the NDF encircles the origin (0,0) in a counterclockwise direction, the determinant  $\Delta$  contains zeroes in the RHP. The number of encirclements is equal to the number of zeroes in the RHP. From Routh [6] and Bode [5], if the determinant of a linear network contains any zeroes in the

#### THE METHOD

The concept of Return Ratio (RR) was first presented by Bode [5] and is defined as the Return Difference minus one or,

$$\text{RR} = \frac{\Delta}{\Delta_0} - 1 \quad (2)$$

where  $\Delta$  and  $\Delta_0$  have been previously defined. The Return Ratio has been used extensively by Maclean [7] to determine stability and assess stability margins of feedback amplifiers. For a network with a single dependent source, the Return Ratio is equivalent to the NDF and can be used as a rigorous check for stability. In this case,

$$\text{NDF} = \frac{\Delta}{\Delta_{Q1}} = \text{RR}_1 + 1 \quad (3)$$

If the network contains more than one dependent source,  $\Delta_{Q1}$  may contain zeroes in the RHP due to other dependent sources, and a single Return Ratio calculation is not sufficient for a rigorous assessment of stability. However, the concept can be extended to networks with N dependent sources by rearranging the previous equation into the form,

$$\Delta = (RR_1 + 1) \Delta_{01} \tag{4}$$

and realizing that,

$$\Delta_{01} = (RR_2 + 1) \Delta_{02} \tag{5}$$

where  $RR_2$  is the Return Ratio of a second dependent source in the network with the first dependent source set to zero. By substituting (5) into equation (4), one can easily see that:

$$\Delta = (RR_1 + 1)(RR_2 + 1) \Delta_{02} \tag{6}$$

By continuous substitution,

$$\Delta = (RR_1 + 1)(RR_2 + 1)(RR_3 + 1) \dots (RR_N + 1) \Delta_{0N} \tag{7}$$

and finally,

$$\frac{\Delta}{\Delta_{0N}} = (RR_1 + 1)(RR_2 + 1)(RR_3 + 1) \dots (RR_N + 1) \tag{8}$$

which is by definition equal to the normalized determinant function NDF equation (1). For a given network, the dependent source Return Ratios may be calculated in any order provided that each successive Return Ratio  $RR_i$  ( $i=2-N$ ) is calculated with all previous dependent sources set to zero. This technique for calculating the NDF can be easily implemented directly inside a circuit simulator such as LIBRA™.

RETURN RATIO CALCULATIONS

The final ingredient necessary to implement our stability method is to calculate the Return Ratio of an arbitrary dependent source embedded in a given linear N-port network. This calculation can be easily accomplished by replacing the dependent source, which is controlled by an internal voltage or current, by an identical source that is controlled by an external voltage or current.

As an example, consider a passively terminated linear N-port network with an embedded dependent source as shown in figure 1 and an identical network where the source is controlled by an external voltage  $v_{ext}$  as shown in figure 2. In this example, the dependent source chosen is a voltage controlled current source. We will show that the Return Ratio of this dependent source is given by:

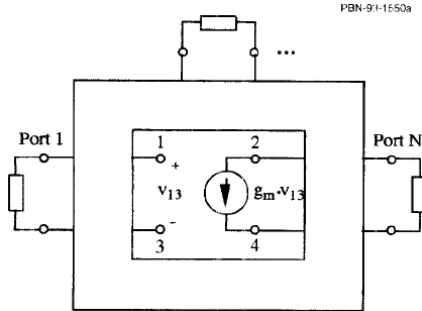


Fig. 1. Passively terminated N-port linear network with an embedded voltage controlled current source.

$$RR = \frac{-v_{13}}{v_{ext}} \tag{9}$$

Equation (9) represents a simple voltage gain calculation and can be performed within any commercial circuit simulator.

To prove equation (9), we start with equation (2) and use the Y parameters of the network shown in figure 1. The Y matrix of the network shown in figure 1 is given by,

$$\begin{bmatrix} Y_{11} & Y_{12} & Y_{13} & Y_{14} & \dots & Y_{1N} \\ Y_{21} + g_m & Y_{22} & Y_{23} - g_m & Y_{24} & \dots & Y_{2N} \\ Y_{31} & Y_{32} & Y_{33} & Y_{34} & \dots & Y_{3N} \\ Y_{41} - g_m & Y_{42} & Y_{43} + g_m & Y_{44} & \dots & Y_{4N} \\ \vdots & \vdots & \vdots & \vdots & \ddots & \vdots \\ Y_{N1} & Y_{N2} & Y_{N3} & Y_{N4} & \dots & Y_{NN} \end{bmatrix} \tag{10}$$

where the first four rows and columns of the matrix represent the four internal nodes (1-4) of the network where the voltage controlled current source is connected. After exchanging rows and columns, the Y matrix can be partitioned as follows,

$$\begin{bmatrix} Y_{21} + g_m & Y_{23} - g_m & Y_{22} & Y_{24} & \dots & Y_{2N} \\ Y_{41} - g_m & Y_{43} + g_m & Y_{42} & Y_{44} & \dots & Y_{4N} \\ Y_{11} & Y_{13} & Y_{12} & Y_{14} & \dots & Y_{1N} \\ Y_{31} & Y_{33} & Y_{32} & Y_{34} & \dots & Y_{3N} \\ \vdots & \vdots & \vdots & \vdots & \ddots & \vdots \\ Y_{N1} & Y_{N3} & Y_{N2} & Y_{N4} & \dots & Y_{NN} \end{bmatrix} \tag{11}$$

or,

$$|Y| = \begin{bmatrix} A & B \\ C & D \end{bmatrix} \tag{12}$$

Using a matrix determinant identity [8], we have,

$$|Y| = \begin{vmatrix} A & B \\ C & D \end{vmatrix} = |A - BD^{-1}C| \cdot |D| \tag{13}$$

and,

$$|Y_0| = \begin{vmatrix} A_0 & B \\ C & D \end{vmatrix} = |A_0 - BD^{-1}C| \cdot |D| \tag{14}$$

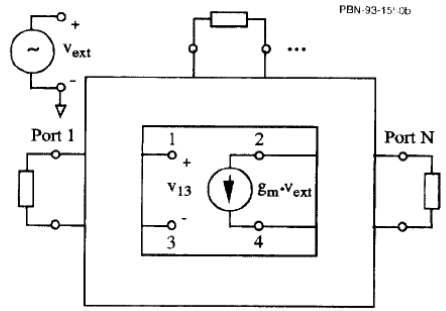


Fig. 2. Passively terminated N-port linear network of figure 1 where the current source is controlled by an external voltage  $v_{ext}$  instead of  $v_{13}$ .

where  $A_0$  represents the sub matrix A with  $g_m$  set equal to zero. Since the sub matrix D in equations (13) and (14) is the same, the Return Ratio  $\Delta / \Delta_0 - 1$  becomes:

$$RR = \frac{|Y|}{|Y_0|} - 1 = \frac{|A - BD^{-1}C|}{|A_0 - BD^{-1}C|} - 1 \quad (15)$$

If we make the following substitutions,

$$\begin{bmatrix} b_{11} & b_{12} \\ b_{21} & b_{22} \end{bmatrix} = BD^{-1}C \quad (16a) \quad A = \begin{bmatrix} a_{11} & a_{12} \\ a_{21} & a_{22} \end{bmatrix} + \begin{bmatrix} g_m & -g_m \\ -g_m & g_m \end{bmatrix} \quad (16b)$$

the Return Ratio is given by:

$$RR = \frac{g_m \{ (a_{11} - b_{11}) + (a_{12} - b_{12}) + (a_{21} - b_{21}) + (a_{22} - b_{22}) \}}{(a_{11} - b_{11})(a_{22} - b_{22}) - (a_{12} - b_{12})(a_{21} - b_{21})} \quad (17)$$

Now, starting from the modified network shown in figure 2, the Y matrix equation is given by:

$$\begin{bmatrix} Y_{11} & Y_{12} & Y_{13} & Y_{14} & Y_{1N} \\ Y_{21} & Y_{22} & Y_{23} & Y_{24} & Y_{2N} \\ Y_{31} & Y_{32} & Y_{33} & Y_{34} & Y_{3N} \\ Y_{41} & Y_{42} & Y_{43} & Y_{44} & Y_{4N} \\ \vdots & \vdots & \vdots & \vdots & \vdots \\ Y_{N1} & Y_{N2} & Y_{N3} & Y_{N4} & Y_{NN} \end{bmatrix} \begin{bmatrix} v_1 \\ v_2 \\ v_3 \\ v_4 \\ \vdots \\ v_N \end{bmatrix} = \begin{bmatrix} 0 \\ -g_m v_{ext} \\ 0 \\ g_m v_{ext} \\ \vdots \\ 0 \end{bmatrix} \quad (18)$$

After exchanging rows and columns, the matrix can be partitioned as follows,

$$\begin{bmatrix} Y_{21} & Y_{23} & Y_{22} & Y_{24} & Y_{2N} \\ Y_{41} & Y_{43} & Y_{42} & Y_{44} & Y_{4N} \\ Y_{11} & Y_{13} & Y_{12} & Y_{14} & Y_{1N} \\ Y_{31} & Y_{33} & Y_{32} & Y_{34} & Y_{3N} \\ \vdots & \vdots & \vdots & \vdots & \vdots \\ Y_{N1} & Y_{N3} & Y_{N2} & Y_{N4} & Y_{NN} \end{bmatrix} \begin{bmatrix} v_1 \\ v_3 \\ v_2 \\ v_4 \\ \vdots \\ v_N \end{bmatrix} = \begin{bmatrix} -g_m v_{ext} \\ g_m v_{ext} \\ 0 \\ 0 \\ \vdots \\ 0 \end{bmatrix} \quad (19)$$

or,

$$\begin{bmatrix} A_0 & B \\ C & D \end{bmatrix} \begin{bmatrix} v_1 \\ v_3 \\ v_2 \\ v_4 \\ \vdots \\ v_N \end{bmatrix} = \begin{bmatrix} -g_m v_{ext} \\ g_m v_{ext} \\ 0 \\ 0 \\ \vdots \\ 0 \end{bmatrix} \quad (20)$$

Note that the partitioned Y matrix in equation (19) is the same as in equation (11) where  $g_m$  is set to zero. Using standard matrix techniques, (20) can be reduced to,

$$[A_0 - BD^{-1}C] \begin{bmatrix} v_1 \\ v_3 \end{bmatrix} = g_m v_{ext} \begin{bmatrix} -1 \\ 1 \end{bmatrix} \quad (21)$$

and solving for  $v_1$  and  $v_3$  gives:

$$v_1 = \frac{-g_m v_{ext} \{ (a_{12} - b_{12}) + (a_{22} - b_{22}) \}}{(a_{11} - b_{11})(a_{22} - b_{22}) - (a_{12} - b_{12})(a_{21} - b_{21})} \quad (22)$$

$$v_3 = \frac{g_m v_{ext} \{ (a_{11} - b_{11}) + (a_{21} - b_{21}) \}}{(a_{11} - b_{11})(a_{22} - b_{22}) - (a_{12} - b_{12})(a_{21} - b_{21})} \quad (23)$$

Subtracting (23) from (22) and dividing by  $v_{ext}$  results in,

$$\frac{-v_{13}}{v_{ext}} = \frac{g_m \{ (a_{11} - b_{11}) + (a_{12} - b_{12}) + (a_{21} - b_{21}) + (a_{22} - b_{22}) \}}{(a_{11} - b_{11})(a_{22} - b_{22}) - (a_{12} - b_{12})(a_{21} - b_{21})} \quad (24)$$

which is equal to equation (17), thus finishing the proof of equation (9). Similar proofs have been done for other dependent sources and the results are presented in Table 1.

	$\alpha \cdot v_{13} \Rightarrow \alpha \cdot v_{ext}$	$RR = \frac{-v_{13}}{v_{ext}}$
	$\beta \cdot i_{13} \Rightarrow \beta \cdot i_{ext}$	$RR = \frac{-i_{13}}{i_{ext}}$
	$\gamma \cdot i_{13} \Rightarrow \gamma \cdot i_{ext}$	$RR = \frac{-i_{13}}{i_{ext}}$
	$\delta \cdot v_{13} \Rightarrow \delta \cdot v_{ext}$	$RR = \frac{-v_{13}}{v_{ext}}$

Table 1. List of dependent sources and their Return Ratio equivalents. Column 2 gives the formula to calculate the Return Ratio of each source from the Return Ratio equivalent.

#### EXAMPLE OF A MMIC APPLICATION

The utility of our method for predicting oscillations in microwave circuits is demonstrated using a two-stage GaAs MMIC amplifier as an example. The layout of the two-stage amplifier is shown in figure 3. Topologically, the amplifier is composed of a parallel connection of two identical two-stage cascades with additional input and output reactively matched sections. Figure 4 shows the corresponding locus of the NDF contour for the two-stage GaAs amplifier. Our method predicts oscillations since the locus of the NDF encircles the origin (0,0) twice. The amplifier was designed and processed prior to the utilization of this method. It was judged to be stable since its stability factor K from input to output was greater than 1 and the determinant of its two-port S parameters was less than 1 in magnitude at all frequencies as shown in figure 5. The fabricated circuit however exhibits very strong oscillations between 8 and 9 GHz and cannot be used as an amplifier at all.

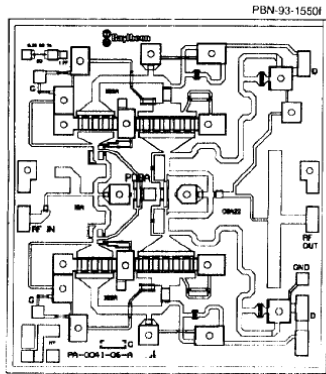


Fig. 3. Layout of a two-stage GaAs MMIC power amplifier.

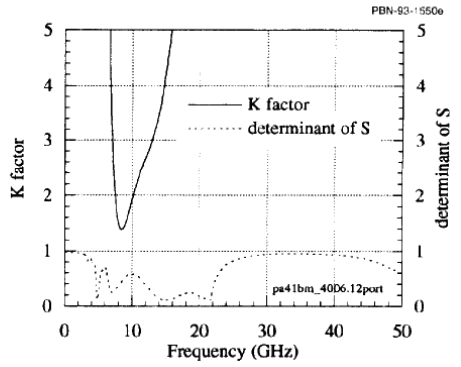


Fig. 5. Plot of K factor and the determinant of S for a two-stage GaAs MMIC power amplifier showing an incorrect prediction of stability.

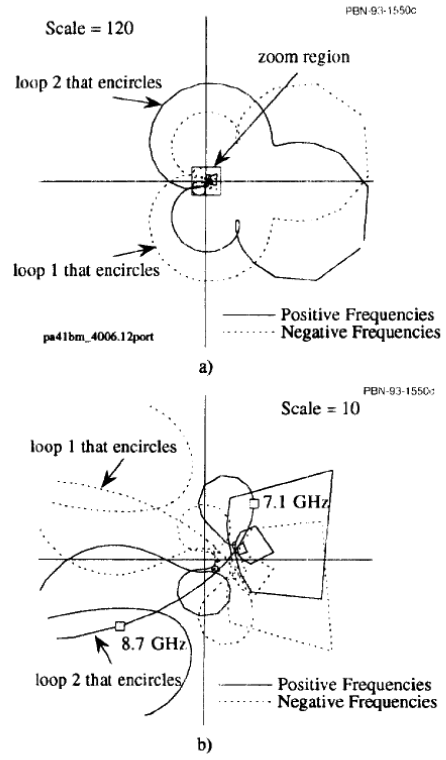


Fig. 4. a) Locus of the normalized determinant function showing instability (two encirclements) for a two-stage GaAs MMIC power amplifier. b) Expanded view of figure 4a (zoom region).

PROPERTIES OF THE NDF

For physically realizable networks, the locus of the NDF over negative frequencies will be a mirror image of the locus over positive frequencies. This means that it will be continuous at both zero frequency and at positive and negative infinite frequencies. Another property of the NDF when applied to physically realizable networks, is that the value of the NDF will always approach (1,0) in value at infinite frequencies. This property is used to determine how high in frequency one must calculate the NDF to guarantee that all possible encirclements of the origin (0,0) have been found.

REFERENCES

- [1] J.G. Linville and L.G. Schimpf, "The Design of Tetrode Transistor Amplifiers", *Bell System Tech. J.*, vol. 35, pp. 813-840, July 1956
- [2] J.M. Rollett, "Stability and Power-Gain Invariants of Linear Two-Ports", *IRE Trans. on Circuit Theory*, vol. CT-9, pp. 29-32, March 1962
- [3] D. Woods, "Reappraisal of the Unconditional Stability Criteria for Active Two-Port Networks in Terms of S Parameters", *IEEE Trans. on Circuits and Systems*, vol. CSA-23, pp. 73-81, February 1976
- [4] A. Platzker, W. Struble, and K. Hetzler, "Instabilities Diagnosis and the Role of K in Microwave Circuits", *IEEE MTT-S Int. Microwave Symposium Dig.*, 1993
- [5] H.W. Bode, "Network Analysis and Feedback Amplifier Design", D. Van Nostrand Co. Inc., New York, 1945
- [6] E.J. Routh, "Dynamics of a System of Rigid Bodies", 3rd Ed., Macmillan, London, 1877
- [7] D.J.H. Maclean, "Broadband Feedback Amplifiers", Research Studies Press, 1982
- [8] Gantmacher, "Matrix Theory", Chelsea Publishing Co., pg. 46, 1959



# Bibliography

- [1] National instruments, microwave office ni awr design environment. [Online]. Available: <http://www.awrcorp.com/products/microwave-office>
- [2] K. Academy. Inverting a 3x3 matrix using determinants. [Online]. Available: <https://www.khanacademy.org/math/precalculus/precalc-matrices/determinants-and-inverses-of-large-matrices/v/inverting-matrices-part-3>
- [3] H. Bode, "Network Analysis and Feedback Amplifier," *D. Van Nostrand Co. Inc., New York*, 1945.
- [4] R. Jackson, "Rollett Proviso in the Stability of Linear Microwave Circuits- A Tutorial," *IEEE Transactions on Microwave Theory and Techniques, Vol. 54, No. 3*, 2006.
- [5] H. Nyquist, "Regeneration theory," 1932.
- [6] A. Platzker and W. Struble, "Instabilities Diagnosis and the Role of K in Microwave Circuits," *IEEE MTT-S Int. Microwave Symposium Dig.*, 1993.
- [7] P. Powell, "Calculating Determinant's of Block Matrices," 2011.
- [8] J. Rollett, "Stability and Power-Gain Invariants of Linear Two-Ports" ,” *IRE Transaction on Circuit Theory, vol CT-9, pp. 29-32*, 1962.
- [9] E. Routh, "Dynamics of a System of Rigid Bodies," *3rd Ed., Macmillan, London*, 1877.
- [10] W. Struble and A. Platzker, "A Rigorous Yet Simple Method for Determining Stability of Linear N-Port Networks," 1994.
- [11] —, "Rigorous determination of the Stability of Linear N-Node Circuits from Network Determinants and the appropriate role of the Stability Factor K of their reduced Two-Ports," 1994.
- [12] E. Tan, X. Sun, and K. Ang, "Unconditional Stability Criteria for Microwave Networks," *Progress in Electromagnetics Research Symposium, Beijing, China*, 2009.
- [13] Wikipedia. Process design kit. [Online]. Available: [https://en.wikipedia.org/wiki/Process\\_design\\_kit](https://en.wikipedia.org/wiki/Process_design_kit)